



HAL
open science

Is normal backwardation normal? Valuing financial futures with a local index-rate covariance

Philippe Raimbourg, Paul Zimmermann

► **To cite this version:**

Philippe Raimbourg, Paul Zimmermann. Is normal backwardation normal? Valuing financial futures with a local index-rate covariance. *European Journal of Operational Research*, 2022, 298 (1), pp.351-367. 10.1016/j.ejor.2021.06.051 . hal-04011013

HAL Id: hal-04011013

<https://hal.science/hal-04011013v1>

Submitted on 8 Jan 2024

HAL is a multi-disciplinary open access archive for the deposit and dissemination of scientific research documents, whether they are published or not. The documents may come from teaching and research institutions in France or abroad, or from public or private research centers.

L'archive ouverte pluridisciplinaire **HAL**, est destinée au dépôt et à la diffusion de documents scientifiques de niveau recherche, publiés ou non, émanant des établissements d'enseignement et de recherche français ou étrangers, des laboratoires publics ou privés.



Distributed under a Creative Commons Attribution - NonCommercial 4.0 International License

Is Normal Backwardation Normal? Valuing Financial Futures with a Local Index-Rate Covariance*

Philippe Raimbourg^a

Paul Zimmermann^{b,c,*}

Abstract

Revisiting the two-factor valuation of futures contracts, we propose a new pricing model for financial futures and their derivatives. The linkage between the money market funding rate and the underlying asset price is stochastic and state-dependent, in compliance with investors' arbitrage strategies. The model explicitly captures the impact of interest rate expectations in the marking-to-market feature of futures, as predicted by Cox, Ingersoll, and Ross's (1981) theory. The backwardation vs. contango regime of financial futures depends on a new parameter, the contango factor, which paves the way for future empirical studies. Akin to the implied volatility of option contracts, the contango factor provides market participants with a universal gauge of futures contracts' level of contango, consistent across futures markets and maturities. Our numerical simulations show significant deviations from the traditional cost-of-carry model of futures prices, with price deviations above 1% even for short-term futures contracts.

JEL classification: G11, G12, G13

Keywords: Finance; Risk management; Futures contracts; Normal backwardation; Stochastic covariance.

Declarations of interest: none

*The authors thank Yann Braouezec, Jean-Paul Laurent, Olivier Le Courtois, Franck Moraux, Nicolas Leboisne, Julien Fouquau (discussant), Ako Doffou (discussant), Kashi Nath Tiwari (discussant), Louis R. Piccotti (discussant), Andrey Ermolov (discussant), and participants at the 2018 AFFI Conference, the 2018 IRMC Conference, the 2018 FMA European Conference, the 2018 World Finance Conference, the 2018 FMA Annual Meeting, the 2018 SFA Conference, and the 2018 Paris December Finance Meeting for helpful comments and suggestions.

^aUniversity Paris 1 Panthéon-Sorbonne, Ecole de Management de la Sorbonne, 1 rue Victor Cousin, 75005, Paris (France).
Email: philippe.raimbourg@univ-paris1.fr

^bIESEG School of Management, 3 rue de la Digue, 59000 Lille, France.

^cLEM-CNRS 9221, 3 rue de la Digue, 59000 Lille, France.

*Corresponding Author. Email: p.zimmermann@ieseg.fr

1. Introduction

Several economic explanations are usually put forward to account for futures risk premiums, defined as the deviations between futures prices and expected future spot prices. Keynes (1930) hypothesizes that speculators claim a premium in exchange for bearing the risk of price fluctuations. This fundamental insight originates the “normal backwardation” theory in which the spot-futures basis arises from the superior forecast power of futures prices. Subsequently, the cost-of-carry hypothesis has built upon the theory of storage (Kaldor, 1939; Working, 1948, 1949) to interpret the spot-futures basis through several technical factors such as storage costs, convenience yields, and interests forgone by storing. After that, the net-hedging-pressure hypothesis has recognized the pressures on futures prices generated by hedging market participants (Cootner, 1960) as a determinant of futures risk premiums. More recently, the literature has emphasized the hedging pressures of both own-market and cross-market hedgers in the determination of futures risk premiums (e.g., Bessembinder, 1992; De Roon, Nijman, and Veld, 2000). Nevertheless, critical empirical studies (e.g., Fama and French, 1987; Kolb, 1992; Laws and Thomson, 2004) have shown that the forecastability pattern of futures prices remains controversial, at the very least.¹

In this article, we build a model that aims to investigate another rationale providing a competing explanation for the futures risk premium of such financial assets as interest-earning assets and stock indexes. Since the seminal works of Black (1976), Jarrow and Oldfield (1981), and Cox, Ingersoll, and Ross (1981), we know that the value of a forward contract is generally not the same as that of a futures contract. Since its costs of marking to market induce regular repayments between the owner and the seller, a futures contract strictly depends, until it matures, on the funding rate prevailing on its holder’s margin account.² The forward and futures prices consequently diverge as soon as interest rates become stochastic. The difference depends on the covariance between the futures prices and the money market account, seen as the natural pricing numeraire of futures contracts. This article revisits the marking-to-market hypothesis, or CIR effect (for Cox, Ingersoll, and Ross), which posits that the market’s expectations of the asset-rate covariance provide the primary driver for the forward-futures price difference.³

In this study, we use two random processes to take into account the specificity of futures contracts. The first relates to the dynamics of the underlying asset price. The second has to do with the evolution of the interest rate term structure. As a characteristic feature of the model, the asset-rate covariance is mainly characterized by (i) being determined by the investors’ arbitrage operations, and (ii) being variable over time, state-dependent, and stochastic. This local arbitrage-free covariance enables our model to capture CIR effects explicitly.

Researchers have long proposed several two- or three-factor models for the valuation of futures contracts. Ramaswamy and Sundaesan’s (1985) two-factor model assumes stochastic interest rates within the Cox, Ingersoll, and Ross (1985) general equilibrium framework. Schwartz (1997) is the first to introduce a three-factor model of futures contracts to capture the stochastic convenience yield of commodities. Miltersen and

¹See Chow, McAleer, and Sequeira (2000) for an extensive survey of the futures pricing literature.

²Lam, Yu, and Lee (2010) discuss the determination by futures clearinghouses of margin rules. More recently, in the aftermath of the financial crisis, the risk-based setting of margin rules in futures markets has received renewed scrutiny from a regulatory perspective (e.g., Alexander, Kaeck, and Sumawong, 2019).

³See the Online Appendix for a survey of the empirical literature on CIR effects.

Schwartz's (1998) three-factor model nests Schwartz's model in the multifactor, non-Markov interest rate framework of Heath, Jarrow, and Morton (1992). Hilliard and Reis (1998) generalize the underlying asset price dynamics to the case of a jump-extended diffusion. The more recent models by Casassus and Collin-Dufresne (2005) and Casassus, Liu, and Tang (2013) use arbitrage-free interest rate diffusions, making possible exact fits to the initial term structure of interest rates. However, the common denominator for all these models is the constant, exogenous correlation between the asset price and the short-term interest rate.

Although the covariance between the underlying asset price and the short-term financing interest rate is generally assumed to be constant over time or to be deterministic, it is well-known that this assumption is not realistic (e.g., French, 1983). Indeed, an old strand in the asset pricing literature has documented the time-varying characteristics of the covariance matrix of asset returns.⁴ From a purely econometric perspective, Gourieroux, Jasiak, and Sufana (2009) advocate for the use of the Wishart autoregressive (WAR) process to model stochastic covariance matrixes. In this vein, Buraschi, Porchia, and Trojani (2010) specify the covariance matrix between S&P 500 futures and Treasury bond futures with a WAR process. Similarly, Chiu, Wong, and Zao (2015) use a WAR process to model the stochastic covariance of co-integrated spot and futures commodities. However, the introduction of a stochastic covariance matrix between several asset price processes ignores the specificity of the asset-rate covariance. By contrast, Driessen, Maenhout, and Vilkov (2009) exploit a simple model-free trading rule to capture the correlation risk premium contained in S&P 100 index options. The arbitrage-free covariance estimator of Brandt and Diebold (2006) suggests an even more parsimonious approach to model stochastic covariance. Following this trend, this article is the first, to the best of our knowledge, to endogenize asset-rate covariances in an arbitrage-free setting. We thereby avoid the theoretical apparatus of an equilibrium framework.⁵

Our valuation framework sheds new light on the "normal backwardation" regime of futures. The index-rate covariance being stochastic and determined by investors' operations, it moves along time and may become negative. In such a situation, an increase in interest rates results in a decrease in both the spot price and the expected future spot price, while the futures price increases as the costs of carrying futures become higher. Due to the conjunction of these two movements, the futures price may cross over the expected future spot price and establish a contango regime.

Our findings are of two kinds: theoretical and empirical. First, by introducing a local covariance, our numerical simulations indicate significant deviations larger than 1% from the traditional cost-of-carry model of futures prices. Our model is thus flexible enough to capture a broad spectrum of configurations for the futures risk premium. It contributes to the extant theoretical literature by leading to reassess the role of the interest rate term structure in the formation of financial futures prices.

Second, we address the practical calibration of the model key parameter. This parameter must be seen as a factor of contango which governs the regime of financial futures and paves the way for future empir-

⁴See, for example, Longin and Solnik (2001).

⁵In parallel to the arbitrage-free approach to futures modeling, some authors have explored equilibrium approaches allowing the correlation structure between risk sources to arise endogenously. Hemler and Longstaff (1991) propose a general equilibrium model of stock index futures prices. Routledge, Seppi, and Spatt (2000) develop a partial equilibrium model of forward prices for storable commodities in which convenience yields arise endogenously as a result of the interaction among supply, demand, and storage decisions. Gorton, Hayashi, and Rouwenhorst (2012) endogenously derive both the spot-future basis and the futures risk premium from the exogenous inventory level.

ical studies. Moreover, this metric is consistent across futures markets and maturities. As an illustration, we analyze the contango factor implied from S&P 500 futures during a period of easing monetary policy (September 2007 to December 2008) and a period of tightening monetary policy (December 2015 to December 2018). We are thus in a position to quantify the significant impacts of the recent U.S. Federal Reserve interest rate hikes on the global regime of S&P 500 futures. This finding should provide decision support to futures market participants engaged in financial strategies such as index arbitrage.

The article proceeds as follows. Section 2 puts forward the model’s microeconomic foundations in a discrete-time setting and builds the arbitrage-free stochastic covariance structure. In Section 4, we conduct an extensive sensitivity analysis of financial futures contracts through numerical simulations. In Section 3, we describe the model calibration process on S&P 500 empirical data. Finally, Section 5 concludes the article. An Online Appendix supplies additional empirical evidence of significant CIR effects in S&P 500 futures risk premiums.

2. The Model

In this section, we build a set of representative economic assumptions to model financial futures contracts and the derivatives written on those assets, such as futures options.

2.1 Conceptual framework

We consider a discrete trading economy of length $[0, T]$ for a fixed $T > 0$. For each trading date $t_i \in [0, T]$, a t_i -maturity discount bond pays a sure dollar at date t_i and trades in a frictionless and complete market. $B_s(t_i)$ denote its time s price for each trading date $s \in [0, t_i]$. We define the money market account, B_t , corresponding to the price of a dollar invested at time 0 and rolled over at the (risk-free) short interest rate, r_t .

We assume that the family $B_s(t_i)$ ($0 \leq t_i \leq T$) is an arbitrage-free family of bond prices relative to the short rate r . In the context of a discrete trading economy, Harrison and Pliska (1981) show that there is no arbitrage opportunity if and only if there exists a probability measure $\tilde{\mathbb{P}}$ making any asset price relative to B_t a martingale. Moreover, market completeness implies the uniqueness of this equivalent martingale measure. For futures pricing purposes, this paper needs only to be concerned with the process for the short rate in the risk-neutral measure. This is because the futures price at horizon T , $F(t, T)$, is the risk-neutral expectation of the underlying asset’s terminal value, $\tilde{\mathbb{E}}_t[S_T]$ (e.g., Cox, Ingersoll, and Ross, 1981).

The choice of a risk-neutral process for the short rate is of primary importance.⁶ Our guiding principle here is to explain the market price of financial futures contracts. For computational purposes, a recombining tree where the number of nodes grows linearly with time should be used to achieve *computational simplicity* in the sense of Nelson and Ramaswamy (1990). As shown by Hull and White (1993), the generalized Vasicek (1977) stochastic dynamics⁷ is a Markov process discretized with trinomial branching and, most

⁶With regard to risk-neutral measures, not all stochastic dynamics for the short-rate process are equally effective. For example, depending on the values of its governing parameters, the CIR square-root process (Cox, Ingersoll, and Ross, 1985) may admit no risk-neutral measure and thus offer arbitrage opportunities (e.g., Heston, Loewenstein, and Willard, 2007).

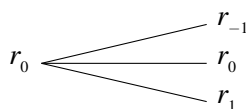
⁷Note that this short-rate process contains no jump that could reflect any harsh modification in the funding cost. For tractability,

importantly, retains computational simplicity. The choice of the discretized model of Hull and White is consistent with the constraint of a unique risk-neutral measure $\tilde{\mathbb{P}}$.

ASSUMPTION 1 (Money market funding cost process). *The money market funding cost is assumed to follow the risk-neutral generalized stochastic dynamics of Vasicek (1977):*

$$dr_t = (h_t - ar_t) dt + v d\tilde{Z}_t, \quad (1)$$

where h_t is a drift term, a is the speed of the mean reversion, v is the interest rate volatility, and \tilde{Z}_t is a Brownian motion under $\tilde{\mathbb{P}}$ driving the term structure movements. The process can be discretized with trinomial branching as follows (Hull and White, 1993):



Notice that in our discrete-time setting, at any date t , the short rate r_t that prevails over the next period $[t, t + 1]$ is known at the beginning of this period.

2.2 A two-factor model

Generally speaking, the link between the evolution of the interest rate term structure and the value of a financial asset remains unclear. To address this problem, we use an arbitrage model whose main characteristic is to assume a stochastic covariance between asset prices and risk-free discount bond prices. The aim is to set up an underlying asset price process that depends on the evolution of the term structure of the money market interest rate.

ASSUMPTION 2 (Risk factors). *The underlying asset price process depends on:*

1. *the changes in the underlying asset's fundamentals (i.e., cash flows);*
2. *the changes in the cost of money reflected by the changes in the money market interest rate, which are equivalent to the funding costs incurred by the holder of a futures contract on her margin account.*

Assumption 2 draws on a long strand in the asset pricing literature. At the firm level, asset price innovations are driven by changes in rational expectations of future cash flow growth and changes in rational expectations of future discount rates (e.g., Campbell and Shiller, 1988a, 1988b; Campbell, 1991; Vuolteenaho, 2002; Hecht and Vuolteenaho, 2006; Chen and Zhao, 2009; Chen, Da, and Zhao, 2013). More precisely, Campbell's seminal paper (1991, Equation 1) shows that unexpected stock returns can be decomposed as:

$$y_{t+1} - E_t y_{t+1} = N_{cf} - N_r, \quad (2)$$

we choose a normally-distributed interest rate diffusion rather than a log-normal diffusion (Black and Karasinski, 1991). Indeed, a normal distribution seems more realistic for futures pricing given central banks' recent monetary policies leading to negative overnight rates.

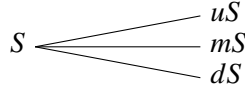
where y_{t+1} is the log return on a stock held from time t to time $t + 1$, E_t denotes a rational expectation at time t , N_{ct} is a news component about future cash flows of the underlying asset, and N_r is a news component about future discount rates. The stock return decomposition (2) should be thought of as a dynamic accounting identity without any behavioral economic content. It provides theoretical support for Assumption 2.

The interest rate dynamics is independent of the underlying asset, but the underlying asset evolution depends on the level of the risk-free rate. Its conditional distribution is then assumed to follow a traditional geometric Brownian motion, which leads to a valuation model of contingent claims identical to the Black and Scholes model (1973).

ASSUMPTION 3 (Asset price process). *The underlying asset price is assumed to follow the subsequent risk-neutral process in a continuous-time setting:*

$$dS_t = (r_t - q_t)S_t dt + \sigma S_t d\tilde{W}_t, \quad (3)$$

where r_t is the (risk-free) interest rate, q_t is the asset continuous dividend yield, σ is the asset volatility, \tilde{W}_t is a Brownian motion under \tilde{P} . The process can be discretized with trinomial branching as follows (Boyle, 1986, 1988):



where u (resp. m , d) is the upward (resp. stable, downward) transition multiplier.

At this stage, we make no binding assumption concerning the correlation between the Brownian motion driving the term structure movements, \tilde{Z}_t , and the Brownian motion driving the underlying asset changes, \tilde{W}_t . We face the same problem as in the Black-Scholes-Merton paradigm for which the volatility parameter σ is not directly observable. The *local volatility* methodology of Dupire (1994), in which the instantaneous volatility is a function of time and spot price $\sigma(t; S_t)$ determined by no-arbitrage conditions, provides the simplest stochastic volatility model to recover all the quoted prices of the options market simultaneously.⁸ Our approach to the instantaneous covariance is similar to the local volatility approach, and we now turn to the specification of this local asset-rate covariance.

2.3 Modeling the asset-rate co-movement

First, we generalize the standard transition multipliers to a joint evolution of the underlying asset's fundamentals and the money market funding cost. Notice that this hybrid evolution takes place under the same risk-neutral probability \tilde{P} as the underlying asset and the short rate.

Definition 1 (Hybrid transition multipliers). $u_n^{j,k}$ (resp. $m_n^{j,k}$, $d_n^{j,k}$) is the evolution coefficient of the underlying asset price between time-steps n and $n + 1$, when a rise (resp. no change, a fall) in the asset's fundamentals occurs, and when the margin account's funding cost transitions from level $j \in \{-n, \dots, n\}$ to level $k \in \{j - 1, j, j + 1\}$.

⁸See Gatheral (2006) for a standard treatment of the local volatility model.

We emphasize that hybrid transitioning captures a covariance-based movement on top of the two distinct moves induced respectively by the underlying asset's fundamentals and the interest rate. If the asset fundamentals and the rate were to move independently, the hybrid transition multiplier would simply write $u_n^{j,k} = u \times (1 - \Delta r)$ where $\Delta r = r_k - r_j$. More often than not, however, the instantaneous asset-rate covariance will not be null. In general, we thus have $u_n^{j,k} \neq u \times (1 - \Delta r)$. This observation motivates us to introduce a new local co-movement factor designed to quantify the impact of the instantaneous asset-rate covariance on the evolution of the underlying asset price.

Definition 2 (Local co-movement factor). *The local co-movement factor $\Phi_n^{j,k}$ captures the movement of the underlying asset price in excess of the asset fundamentals and the interest rate:*

$$\Phi_n^{j,k} := \frac{u_n^{j,k}}{u(1 - \Delta r)}, \quad (4)$$

where the interest rate transitions from level $j \in \{-n, \dots, n\}$ to level $k \in \{j - 1, j, j + 1\}$. Assuming that the modifications are identical whether the fundamentals' scenario proves to be bullish, bearish or stable, the co-movement factor writes similarly:

$$\Phi_n^{j,k} = \frac{d_n^{j,k}}{d(1 - \Delta r)}, \quad \left(\text{resp. } \Phi_n^{j,k} = \frac{m_n^{j,k}}{1 - \Delta r} \right). \quad (5)$$

To understand the intuition behind the previous definition, assume for the moment that the joint distribution of the random vector $(\Delta S/S, \Delta r)$ is the bivariate normal distribution. In this specific case, the following result shows that the local co-movement factor becomes an explicit function of the instantaneous asset-rate covariance as expected.

PROPOSITION 1. *Assume that the joint distribution of the random vector $(\Delta S/S, \Delta r)$ is the bivariate normal distribution. The local co-movement factor is then given by:*

$$\Phi = 1 + \text{Cov} \left[\frac{\Delta S}{S}, \Delta r \right] \times \frac{\Delta r - \tilde{\mathbb{E}}[\Delta r]}{\text{Var}[\Delta r]}. \quad (6)$$

Proof. See Appendix A. □

Equation (6) captures the excess covariance of the underlying asset and the interest rate relative to the covariance of their fundamentals, that is, the “co-movement” between the two asset classes.⁹ Notice how it tends to one as soon as the covariance shrinks to zero. The co-movement factor Φ may reflect, for example, the activity of liquidity traders allocating funds in and out of the two asset classes. It may also reflect the feedback effect of a derivatives market in which participants incorporate information about future fees paid for deferring trade settlements.

We stress that Equation (6) is specific to the case of the bivariate normal distribution. In the general case, however, Equation (6) only provides a prototype for the definition (4-5) of Φ and the economic rationale for

⁹See Veldkamp (2006) for an information-based theory of co-movement where assets co-move as soon as investors price them with a common subset of information. See also Barberis, Shleifer, and Wurgler (2005) for friction- or sentiment-based theories.

it. In the rest of the paper, it will be natural to view the co-movement factor as “gluing” the cash-flow news component to the discount-rate news component as follows:

$$u_n^{j,k} \approx u \cdot \Phi_n^{j,k} \cdot \frac{1+r_j}{1+r_k}, \quad (7)$$

where we have used $1 - \Delta r = 1 + r_j - r_j - \Delta r \approx (1 + r_j)(1 - r_j - \Delta r) \approx (1 + r_j)/(1 + r_j + \Delta r)$ at first order.¹⁰ Notice how each co-movement factor is specific to an interest rate scenario, which leads to a *state-dependent* asset-rate covariance. We make no assumption either about the values of the parameters Φ , or about the relationship that could exist between them. They may be, notably, superior or inferior to unity and therefore dampen or accelerate the movement caused by the variation in the interest rate. In particular, if the interest rate remains constant, we assume a neutral co-movement factor equal to one (i.e., $\Phi_n^{j,j} \equiv 1$).

A simple heuristic argument shows why the futures price should be an increasing function of the co-movement factor. Let us consider the case of an upward movement of the underlying asset’s *fundamentals* ($u > 1$) caused by positive news about future cash flows. Simultaneously, let us consider the *ex-post* profit on a long futures position generated by the concomitant rise in the futures price ($u_n^{j,k} > 1$) that should ensue. Now, notice that everything else being equal in Equation (7), the co-movement factor Φ and the funding rate r_k should move in the same direction. With a co-movement factor above (below) one, the futures holder’s margin account should thus remunerate profits at a higher (lower) funding rate than with a neutral co-movement factor, say equal to one. From an *ex-ante* perspective, the theoretical futures price should consequently be higher (lower) when market participants expect co-movement factors above (below) one. This mechanism should lead in practice to a contango regime in which the futures price evolves above the expected future spot price.

The line of reasoning would be the same for the opposite case of a downward movement of the underlying asset’s *fundamentals* ($d < 1$) caused by negative news about future cash flows. The corresponding *ex-post* profit on a short futures position would be magnified by a higher funding rate generated by a higher co-movement factor. From an *ex-ante* perspective, market participants will trade at higher futures prices when they expect co-movement factors to rise above one, thereby spurring a contango regime to establish.

Note that the previous arguments are set up “everything else being equal,” particularly as the asset and futures respective values do not change. But when the spot-futures basis moves, the factor Φ and the funding rate r no longer develop in the same direction. In practice, many confounding effects will prevent the observation in the data of such a direct relationship between Φ and r .

2.4 A hybrid recombining lattice

When affected by the combined influence of fundamentals and money market interest rates, the underlying asset price evolves according to a multinomial lattice.

ASSUMPTION 4 (Multinomial lattice convergence). *When the money market interest rate stays at its initial level, the multinomial lattice joins the classical trinomial model specified for the marginal evolution of the underlying asset.*

¹⁰For simplicity, the short rate r is not expressed in annual rate but over the Δt period.

Assumption 4 ensures that the hybrid lattice joins the underlying asset's trinomial lattice when the margin account funding cost stays at its initial level (i.e., at $j = 0$). Consequently, we fix the following values:

$$\begin{cases} u_n^{0,0} = u, \\ m_n^{0,0} = 1, \\ d_n^{0,0} = u^{-1}. \end{cases} \quad (8)$$

The next assumption comes from the observation that most of the time, options on financial futures are American-style derivatives. Indeed, due to the very nature of futures contracts, which are usually closed out before reaching maturity, derivatives on futures are inherently subject to premature exercise. As a result, the underlying asset price process should preferably be a Markov process represented by a recombining lattice whose number of nodes grows linearly with the time variable (Nelson and Ramaswamy, 1990).

ASSUMPTION 5 (Hybrid lattice recombination). *At least two different paths may reach any node inside the multinomial lattice.*

Assumption 5 imposes constraints on the structure of the co-movement factor.

- *Reflexivity.* If the lattice is to recombine, we must have $m_n^{j,j} \equiv 1$ for all $j \in \{-n, \dots, n\}$, and then:

$$\Phi_n^{j,j} = 1. \quad (9)$$

- *Symmetry.* If the lattice is to recombine, we must have $u_n^{j,j+1} \cdot d_n^{j+1,j} \equiv 1$ for all $j \in \{-n, \dots, n\}$, and then:

$$\Phi_n^{j,j+1} \cdot \Phi_n^{j+1,j} = \Phi_n^{j,j-1} \cdot \Phi_n^{j-1,j} = 1. \quad (10)$$

More generally, Assumption 5 enables to extend the definition of the co-movement factor to one-step transitions between non-adjacent levels of the interest rate in a consistent way. For example, $\Phi_n^{j,j+2}$ must be understood as the product $\Phi_n^{j,j+1} \cdot \Phi_n^{j+1,j+2}$, even though one-step transitioning from level j to level $j+2$ happens with probability zero. Finally, in the sequel, we make extensive use of the vector $\{\Phi_n^{0,k}\}_{k \in \{-n, \dots, n\}}$ as the hybrid lattice's coordinate system. We thus define the numbers $\Phi_n^{0,k}$ (resp. $\Phi_n^{0,-k}$) for all $k \in \{0, \dots, n\}$ through the following *chain rule*:

$$\Phi_n^{0,k} := \Phi_n^{0,1} \times \Phi_n^{1,2} \times \dots \times \Phi_n^{k-1,k}, \quad \left(\text{resp. } \Phi_n^{0,-k} := \Phi_n^{0,-1} \times \dots \times \Phi_n^{-k+1,-k} \right). \quad (11)$$

2.5 Determining the local co-movement factor

We follow a promising trend in the literature on correlation modeling (Brandt and Diebold, 2006; Driessen, Maenhout, and Vilkov, 2009). Here, we let the principle of absence of arbitrage determine the parametric structure of co-movement factors. As shown by the following technical proposition, it turns out that this crucial financial consideration is constraining enough to build the whole matrix $\{\Phi_n^{0,k}\}_{n,k}$. As a result, at each time-step n , the economic modeling of the asset-rate covariance finds itself fully encapsulated in a single seeding value $\Phi_n^{0,1}$ of the co-movement vector $\{\Phi_n^{0,k}\}_k$.

PROPOSITION 2 (Local co-movement factor).

(a) Under the absence of arbitrage, the following relationship holds:

$$\Phi_n^{0,-1} = a_{n,0} + b_{n,0} \cdot \Phi_n^{0,1}, \quad (12)$$

where the coefficients $a_{n,0}$ and $b_{n,0}$ depend exclusively on r_0 , $r_{\pm 1}$, the underlying asset price diffusion parameters u , m , and d , as well as the money market funding costs.

(b) More generally, for all time steps n and all levels k of the short rate, the absence of arbitrage opportunity leads to the following relationship:

$$\Phi_n^{k,k-1} = a_{n,k} + b_{n,k} \cdot \Phi_n^{k,k+1}, \quad (13)$$

where the coefficients $a_{n,k}$ and $b_{n,k}$ depend exclusively on the short rate at levels k , $k \pm 1$, the underlying asset price diffusion parameters u , m , and d , as well as the term structure of the money market funding cost.

(c) As a result, given the single value of the co-movement factor $\Phi_n^{0,1}$, the co-movement vector $\{\Phi_n^{0,k}\}_{k \in \{-n, \dots, n\}}$ becomes fully determined thanks to the Equation (13).

Proof. See Appendix B. □

2.6 The stochastic asset-rate covariance

The evolution of the asset price depends on two interdependent random processes, the underlying asset's fundamentals and the money market funding cost. As shown by [Proposition 1 in the case of the normal bivariate distribution](#), it is possible to obtain the expression for the instantaneous covariance between the asset price percentage change and the interest rate change. It depends, notably, on the local co-movement factor structure, that is, on the [asset fundamentals](#) and interest rate processes. As a consequence, the asset-rate covariance process is stochastic, which appears to be a sensible economic assumption when it comes to pricing futures contracts. [We now generalizes this result to the non-Gaussian case.](#)

PROPOSITION 3 (Stochastic covariance). *The covariance process between the dynamics of the underlying asset's fundamentals and the dynamics of the money market funding cost is stochastic. Moreover, we have at node $(n; i, j)$:*

$$\tilde{\mathbb{E}}[\Phi] = 1 + k \cdot \text{Cov} \left[\frac{\Delta S}{S}, \Delta r \right] + O(\Delta r), \quad (14)$$

where $k = \left((q_u^{n,j} u + q_m^{n,j} m + q_d^{n,j} d) \Delta r \right)^{-1} > 0$. When the spatial resolution of the hybrid lattice decreases ($\Delta r \downarrow 0$), the sign of the instantaneous asset-rate covariance is given at first order by $\tilde{\mathbb{E}}[\Phi] - 1$, that is, the distance of the expected local co-movement factor to one.

Proof. See Appendix C. □

Notice that Equation (14) is the non-Gaussian counterpart of the exact relationship given by Equation (6) in the Gaussian case. Put differently, the asymptotic contribution $O(\Delta r)$ is the price to pay for dropping any distributional assumption.

2.7 The co-movement factor and the determination of the regime of futures

Recall that a futures contract is said to be in normal backwardation (resp. contango) when the futures price is below (resp. above) the expected future spot price at maturity. The following result provides a *sufficient* condition for a contango regime to establish.

PROPOSITION 4 (Contango regime). *Let assume that the underlying asset makes no discrete payouts. The difference between the futures and forward prices, $F(t, T) - G(t, T)$, is always equal to the value at time t of the following stream of payments:*

$$v^2 \tau_a^2 \sum_{i=t}^{T-1} \frac{S_i B_T}{B_i(T)} + \tau_a \sum_{i=t}^{T-1} \frac{\tilde{E}_i[S_{i+1}] B_T}{B_i(T)} \left(\tilde{E}_i[\Phi_{i+1}] - 1 \right) \Delta r + O(\Delta r^2), \quad (15)$$

where $B_i(T)$ is the price at time i of a default-free discount bond paying one dollar at time T , B_T is the money market account at time T , and $\tau_a = (1 - e^{-a(T-t)})/a$ is a characteristic time. Moreover:

- (a) For the futures price to exceed the expected future spot price (contango regime), it is sufficient that all risk-neutral expectations of future co-movement factors exceed one (i.e., $\tilde{E}[\Phi] \geq 1$).
- (b) Conversely, for the expected future spot price to exceed the futures price (backwardation regime), it is necessary that the risk-neutral expectation of the future co-movement factor falls below one (i.e., $\tilde{E}_n[\Phi_n] \leq 1$ for at least one time-step n).

Proof. See Appendix D. □

We should notice that a sufficient condition characterizes a contango regime, whereas a necessary condition stems from the backwardation regime, meaning the boundary between the two regimes is not exactly $\tilde{E}[\Phi] \equiv 1$ but is slightly lower than one. Equation (15) shows that this boundary depends primarily on the asset value, the interest rate variance, and a proxy of futures' duration. Looking jointly at Propositions 3 and 4 makes it evident that a backwardation regime always goes with a negative asset-rate covariance, whereas a positive covariance always means a contango regime.

We now turn back to the designation of the co-movement parameter Φ as a “contango factor.” Following tradition, we shall refer to the term *contango*, a term commonly used on the London Stock Exchange until the 1930s to designate the seller's remuneration for carrying the asset and deferring its delivery to the buyer.¹¹ Proposition 4 shows that our terminology is fully consistent with the one commonly used in futures markets.

¹¹First recorded in the mid-1800s in England, the term is considered to be an alteration of either the word *continuation*, the word *continue*, or the word *contingent*.

2.8 Pricing futures contracts

The contractual futures price is the delivery price for which the value of the futures contract is zero. It is not the value of a financial asset in itself, as first noticed by Cox, Ingersoll, and Ross (1981). As such, we cannot directly evaluate futures prices in our arbitrage-free framework. However, as recognized by the same authors (cf. Proposition 7, p. 327), the inception price of a futures contract is also the value of a specific financial asset that would pay the underlying asset price at maturity, as well as a continuous flow of the prevailing spot rate times the current futures price from inception up to the contractual maturity. This asset is no different from the underlying asset paying an extra continuous dividend at the money-market, risk-free rate. The current framework, whose numeraire is the money market account, enables us to value this new asset easily.

In [Appendix E](#), we describe a lattice-based implementation of the model. In this discrete-time valuation framework, we obtain the desired futures price by regular backward induction of the underlying asset terminal price, as soon as we cease to discount the cash-flows at each time-step of the hybrid lattice.

2.9 Discussion of model assumptions

Futures contracts are essential for financial markets due to their use as a hedging instrument. Researchers have highlighted futures contracts's role in downside risk reduction (e.g., Lien and Tse, 1998, 2002). Futures hedge ratios based on one-sided risk measures such as lower partial moments (Fishburn, 1977; Bawa and Lindenberg, 1977) have been proposed to formulate optimal hedging strategies (e.g., Chen, Lee, and Shrestha, 2003). They seem more consistent with managers' perception of risks associated with below-target returns. However, as we follow Cox, Ingersoll, and Ross's (1981) central insight that the second centered moment (variance) is the key driver of the futures-forward price deviation, this asymmetric response in the market is not captured in our model.

Why choosing to impart a mean-reverting drift to the short rate dynamics? Our modeling choice is primarily motivated by its mathematical tractability. As explained in [Appendix E.3](#), the hybrid lattice's non-explosive aspect arises from the mean-reverting feature of the short rate dynamics. Moreover, there are profound economic arguments for interest rates reverting to the mean.¹² However, the mean-reversion of rates entails another limitation of our model related to the time variation in the underlying asset's return rate. The reader should notice that the risk neutrality assumption forces the expected return to coincide with the interest rate r . As the interest rate's stochastic process is reverting to a long-term mean, the underlying asset finds itself equipped with a stable mean process under the risk-neutral measure. However, the asset pricing literature has shown that cyclical variation in stock market volatility is often offset by cyclical variation in expected returns (e.g., Whitelaw, 1994). This feature is not captured in our model.

¹²Interest rates are instrumental in bringing investments and savings back to equilibrium. When rates are high, investing will be more expensive, prodding central banks to decrease rates. Conversely, when rates are low, investing will be cheaper, spurring central banks to raise interest rates to avoid overheating of the economy.

3. Calibration of the Contango Factor

In this section, we test the robustness of our discrete-time model by calibrating the contango factor against the closing price histories of the S&P 500 futures contract and its underlying cash index.

3.1 The S&P 500 spot-futures basis

We consider the S&P 500 stock market index, which underlies the world’s most heavily traded stock index futures contracts. S&P 500 futures have recently evolved in a context of (i) rising interest rates on the money market caused by the U.S. Federal Reserve’s recent monetary policy tightening, and (ii) carrying costs being uniform across futures expiries. Indeed, the S&P 500 index enjoys a broad and diversified base of quarterly-dividend-paying stocks, which leads to predictable carrying costs over the year.

Spot and futures prices are taken from Thomson Reuters and expressed in index points.¹³ We consider daily observations from two distinct and complementary sample periods. The first two-year sample period (2007-2008) covers the financial crisis and the subsequent monetary easing cycle. By contrast, 2015-2018 represents a four-year sample period marked by a gradual tightening of monetary policy for the S&P 500. Although a stock index futures contract may be opened up to a year before its delivery month,¹⁴ market participants predominantly invest in the first nearby (or “front month”) contract and then roll into the next nearby contract over the few days preceding its expiration date. Consequently, we limit the observations to the four months (ca. 82 daily observations) of active trading before the rollover date, the only period during which significant open interest¹⁵ appears on the futures contract.

Panel A of Table 1 reports summary statistics for the daily S&P 500 spot-futures basis, $S(t) - F(t, T)$. We observe a slightly increasing (decreasing) trend in the mean of the spot-futures basis over the first (second) sample period. The standard deviation of the daily spot-futures basis is low and does not differ much across contracts. To assess the normality of the spot-futures basis distribution, we report sample estimates for the skewness and the kurtosis. Given the small sample size ($n = 82$), p -values for normality tests have been computed by Monte-Carlo simulation with 10,000 samples. For most futures contracts, we observe departures from normality through significant positive skewness (8 contracts out of 24) or significant excess kurtosis (12 contracts out of 24) at the 5% level. The omnibus K^2 statistic combining sample skewness and kurtosis (D’Agostino and Pearson, 1973) confirms these deviations (unreported for brevity). Only half of the futures contracts exhibit an omnibus statistic that is not significant at the 5% threshold, thereby hinting at actual normal distributions.

To assess the basis’s trend-stationarity, we run an augmented Dickey-Fuller (ADF) unit root test (Dickey and Fuller, 1981) with a constant and time trend for each futures contract. As unit root tests notoriously lack statistical power in small samples to detect unit roots and distinguish between drift and trend, we jointly

¹³In this paper, we use quotes and volume data for the electronically-traded E-Mini S&P 500 futures contract (\$50 per index point), which is more liquid than the standard-size S&P 500 futures contract (\$250 per index point) that still trades via exchange pits. Note that the Chicago Mercantile Exchange’s daily settlement procedure (3:15 pm Chicago time) ensures that both contracts share the same settlement price exactly.

¹⁴Expirations for stock index futures contracts usually occur on the third Friday of the delivery months which follow a quarterly expiration cycle (i.e., March, June, September and December).

¹⁵The open interest of a futures contract is the number of outstanding contracts that have not been closed by an offsetting trade.

perform a KPSS stationarity test (Kwiatkowski et al., 1992) of the null hypothesis of stationarity around a time trend. Panel A of Table 1 shows that the ADF test statistic τ_τ consistently rejects the unit root hypothesis at the 1% level. At the same time, the KPSS test statistic η_τ never rejects the trend stationarity hypothesis. Moreover, both unit root tests and stationarity tests coincide with evidence for the presence of a time trend in the data. This joint evidence wards off the prospect of stochastic trends in the S&P 500 daily spot-futures basis.

3.2 Model calibration to the spot-futures basis

To assess the performance of our valuation model, we compare the model's theoretical price to the market quoted price, $F_{\text{market}}(t, T)$, and estimate the following *mispricing* function:

$$\Delta F := F_{\text{model}}(S(t), \Phi^{0,1}, T, r_t, d_{t,T}, \sigma, \nu, a) - F_{\text{market}}(t, T), \quad (16)$$

where σ, ν and a are the diffusive parameters of the model, r_t is the interest rate term structure, and $d_{t,T}$ is the dividend forecast for horizon T seen from date t . However, depending on the futures contract maturity and the market conditions, the magnitude of this mispricing may be challenging to interpret. We circumvent this methodological difficulty by calibrating the parameter $\Phi^{0,1}$ such that $\Delta F \equiv 0$ to map the mispricing into the contango factor metrics.¹⁶

Consider the model's theoretical price as a function of the contango factor :

$$F_\Phi : \Phi \longmapsto F_{\text{model}}(S(t), \Phi, T, r_t, d_{t,T}, \sigma, \nu, a).$$

This function is monotonic (see Section 4.1) and can be inverted to obtain the market-implied contango factor $\tilde{\Phi} := F_\Phi^{-1}(F_{\text{market}})$ as the value of the parameter $\Phi^{0,1}$ such that the model yields the closing futures price for the given simultaneous closing price of the cash index:

$$F_{\text{model}}(S(t), \tilde{\Phi}(t, T), T, r_t, d_{t,T}, \sigma, \nu, a) = F_{\text{market}}(t, T). \quad (17)$$

As an explicit function of simultaneous closing spot and futures prices, the market-implied contango factor is also an implicit function of the spot-futures basis. Notice how the quantity $\tilde{\Phi}(t, T)$ subsumes the daily level of the spot-futures basis altogether with the market's interest rate expectations. Akin to the implied volatility of option contracts, the market-implied contango factor provides market participants with a universal gauge of the level of contango that is consistent across futures markets and maturities.

The calibration of the market-implied contango factor entails some assumptions regarding the estimation of the cost of carrying stock index futures. First, we estimate the cost of carrying front-month futures using the index of dividend points effectively realized by the underlying cash index. The cost of carrying the front-month contract may be assumed to be deterministic in a first approximation because the three-month period between rollover dates is the only period during which significant open interest appears. Indeed, as dividend

¹⁶The situation is analogous to the one prevailing in options markets where practitioners measure option price differences in terms of implied volatility against the sensitivity (vega) of their pricing model.

Table 1. Descriptive statistics

This table reports summary statistics for the daily S&P 500 spot-futures basis (Panel A), $S(t) - F(t, T)$, and the daily market-implied contango factor, $\tilde{\Phi}(t, T)$ (Panel B). On each trading day, we have calibrated the contango factor against the closing prices of the E-Mini S&P 500 futures contract and the S&P 500 cash index. The cumulated index of annual realized dividend points has provided a proxy for the cost of carrying futures contracts. Overnight, 1-week, 1-month, 2-month, and 3-month tenors of LIBOR have provided proxies for the USD money market. Constant volatility parameters have been used to diffuse the interest rate process ($v = 0.001$, $a = 0.1$). The S&P 500 stock index realized volatility is estimated with an EWMA historical estimator. τ_τ is the ADF test statistic for the null of a unit root process with a constant and time trend. Exact p -values for skewness (Skew) and kurtosis (Kurt) have been calculated by Monte-Carlo simulation with 10,000 samples. η_τ is the KPSS test statistic for the null of stationarity around a time trend. ***, ** and * denote statistical significance at the 1%, 5%, and 10% levels, respectively. Sample periods: (a) December 2006 to December 2008, (b) December 2014 to December 2018. Data source: Thomson Reuters.

Contract	Panel A: $S(t) - F(t, T)$								Panel B: $\tilde{\Phi}(t, T)$								Obs.
	Min	Mean	Max	SD	Skew	Kurt	τ_τ	η_τ	Min	Mean	Max	SD	Skew	Kurt	τ_τ	η_τ	
Mar. 07	-17.5	-8.4	3.0	5.2	0.06	-1.01**	-5.26***	0.06	0.889	0.896	0.904	0.003	0.09	0.68	-3.99**	0.15	82
Jun. 07	-17.2	-8.4	1.5	4.8	0.02	-0.84*	-6.41***	0.09	0.881	0.896	0.902	0.003	-1.85***	8.41***	-5.80***	0.12	82
Sep. 07	-19.4	-8.8	2.6	5.8	-0.06	-1.12**	-6.17***	0.16	0.886	0.896	0.910	0.004	0.16	1.28**	-4.95***	0.16	82
Dec. 07	-18.9	-7.7	13.7	6.4	0.61**	0.64	-3.86**	0.08	0.888	0.904	0.916	0.006	-0.06	-0.47	-4.58***	0.05	82
Mar. 08	-15.3	-5.2	5.6	5.4	-0.19	-1.18**	-4.46***	0.12	0.886	0.925	0.959	0.017	0.04	-1.22**	-5.13***	0.10	82
Jun. 08	-7.0	-1.4	6.6	2.8	0.33	0.19	-7.02***	0.06	0.922	0.934	0.943	0.005	-0.40	-0.65	-4.77***	0.10	82
Sep. 08	-5.8	-0.5	7.3	2.2	0.71***	1.36**	-4.75***	0.16	0.913	0.927	0.947	0.007	0.46*	0.10	-3.05	0.16	82
Dec. 08	-12.9	-0.9	13.4	5.4	0.30	0.08	-5.86***	0.09	0.882	0.927	0.965	0.016	-0.18	0.13	-4.20***	0.16	82
Mar. 15	-7.0	5.1	17.5	3.9	0.01	1.05**	-6.13***	0.08	0.959	0.973	0.987	0.008	0.15	-1.19**	-6.33***	0.10	82
Jun. 15	-2.9	5.5	14.2	3.9	-0.19	-0.75	-5.81***	0.13	0.958	0.971	0.986	0.008	0.17	-1.12**	-5.23***	0.12	82
Sep. 15	-6.4	5.7	22.7	4.2	0.43*	2.60***	-5.68***	0.10	0.955	0.970	0.987	0.008	0.30	-0.69	-5.50***	0.10	82
Dec. 15	-4.8	7.0	31.7	5.6	0.81***	3.49***	-6.55***	0.09	0.934	0.967	0.983	0.009	-0.46*	0.74	-6.54***	0.05	82
Mar. 16	-3.7	6.7	18.9	4.4	0.06	-0.10	-5.88***	0.15	0.936	0.956	0.978	0.011	0.38	-0.97**	-4.81***	0.18	82
Jun. 16	-0.6	6.4	21.2	4.1	0.78***	0.92**	-8.48***	0.11	0.939	0.961	0.975	0.008	-0.29	-0.73	-9.25***	0.15	82
Sep. 16	-5.0	6.0	19.2	4.6	0.32	0.28	-8.33***	0.10	0.945	0.959	0.972	0.007	-0.27	-1.09**	-7.83***	0.13	82
Dec. 16	-1.8	5.4	13.3	3.4	-0.09	-0.66	-7.37***	0.19	0.943	0.956	0.969	0.007	0.08	-1.14**	-8.01***	0.15	82
Mar. 17	-2.9	4.2	9.8	2.6	-0.31	0.06	-5.03***	0.10	0.943	0.954	0.967	0.006	0.06	-0.90*	-5.26***	0.08	82
Jun. 17	-2.5	3.3	9.6	2.4	0.27	-0.45	-5.75***	0.10	0.944	0.954	0.966	0.006	0.50*	-0.87*	-2.99	0.18	82
Sep. 17	-3.8	2.0	6.3	2.0	-0.30	-0.24	-5.71***	0.09	0.944	0.954	0.967	0.006	0.23	-0.95**	-5.17***	0.15	82
Dec. 17	-3.5	1.9	6.6	2.1	-0.20	0.16	-5.49***	0.12	0.943	0.952	0.962	0.004	0.10	-0.49	-5.29***	0.09	82
Mar. 18	-16.2	-0.5	28.4	5.2	2.02***	11.47***	-4.64***	0.07	0.928	0.947	0.961	0.004	-0.88***	6.96***	-4.90***	0.07	82
Jun. 18	-14.8	-1.9	9.9	3.9	-0.51**	1.47**	-4.23***	0.12	0.931	0.939	0.947	0.004	0.51*	-0.27	-3.03	0.18	82
Sep. 18	-9.7	-2.2	8.0	2.9	0.76***	2.17***	-5.80***	0.15	0.928	0.936	0.945	0.004	0.22	-1.12**	-5.63***	0.14	82
Dec. 18	-19.6	-3.0	24.1	6.6	1.25***	3.72***	-7.66***	0.08	0.914	0.933	0.945	0.005	-0.86***	3.57***	-7.14***	0.08	82

uncertainty quickly resorbs when moving closer to the delivery date, the dividend forecast $d_{t,T}$ expected by futures arbitrageurs adjusts with the dividend yield that is effectively realized by the stock market index. Second, we perform all calibrations with the same volatility and mean-reversion parameters v and a for the interest rate diffusion. Using uniform diffusive parameters ensures a consistent calibration of $\tilde{\Phi}$ across all dates.

3.3 The market-implied contango factor

Figure 1 displays the market-implied contango factor $\tilde{\Phi}$ for the S&P 500 futures contract expiring in March 2017. On each trading day, we have calibrated $\tilde{\Phi}$ against the futures and cash index closing prices. In a sign of model robustness, the calibration shows very little sensitivity to the levels of cash index volatility and interest rate volatility. This robustness leads to calibrate with standard values for the interest rate diffusion parameters ($v = 0.001$, $a = 0.1$). To neutralize the impact of the S&P 500 stock index volatility further, we have used an exponentially weighted moving average (EWMA) estimator, which tracks the changes in the S&P 500 realized volatility closely.¹⁷ Finally, as relevant proxies of the USD money market for the two periods considered in our historical calibration, we have used the short tenors of LIBOR interest rates (overnight, 1 week, 1, 2, and 3 months).¹⁸

Figure 1a plots the daily spot-futures basis, $S(t) - F(t, T)$, in which the high cost of carrying futures may explain the apparent regime of normal backwardation. In parallel, Figure 1b shows the implied contango factor $\tilde{\Phi}(t, T)$ increasing slowly toward one, in line with Proposition 4 and our numerical simulations, which predict a contango factor less than one in case of normal backwardation of futures prices (see Section 4.1). However, a secondary effect may be advanced to explain the convergence of $\tilde{\Phi}(t, T)$ toward one as the contract delivery is nearing ($t \uparrow T$). Because the residual time to maturity of the futures contract shrinks to zero, the expected interest charges credited on the futures holder's margin account have less and less duration. As a result, the negative covariance between the underlying cash index and the overnight interest rate exerts a receding impact upon the futures price's formation.¹⁹

Panel B of Table 1 reports summary statistics for the daily contango factor $\tilde{\Phi}$ implied from the S&P 500 spot-futures basis over the 24 contracts covered by our two sample periods. Generally speaking, $\tilde{\Phi}$ appears to be stable along time, with low standard deviations. While skewness is almost nonexistent (except for three contracts out of 24), significant excess kurtosis at the 5% threshold appears almost as frequently (12 contracts out of 24) as for the S&P 500 spot-futures basis. The (unreported) omnibus K^2 statistic combining sample skewness and kurtosis (D'Agostino and Pearson, 1973) shows the same proportion of actual normal

¹⁷The EWMA weighting scheme is given by $\sigma_t^2 = \lambda \sigma_{t-1}^2 + (1 - \lambda) u_t^2$, where u_t is the underlying asset's current log-return, and the weighting parameter $\lambda = 0.94$ corresponds to a half-life equal to $\ln(0.5) / \ln(\lambda) \approx 11$ (trading) days.

¹⁸As the typical interest rate at which large banks lend on an unsecured basis to other banks, LIBOR interest rates provide a closer proxy of the funding costs incurred by the marginal investor in futures contracts.

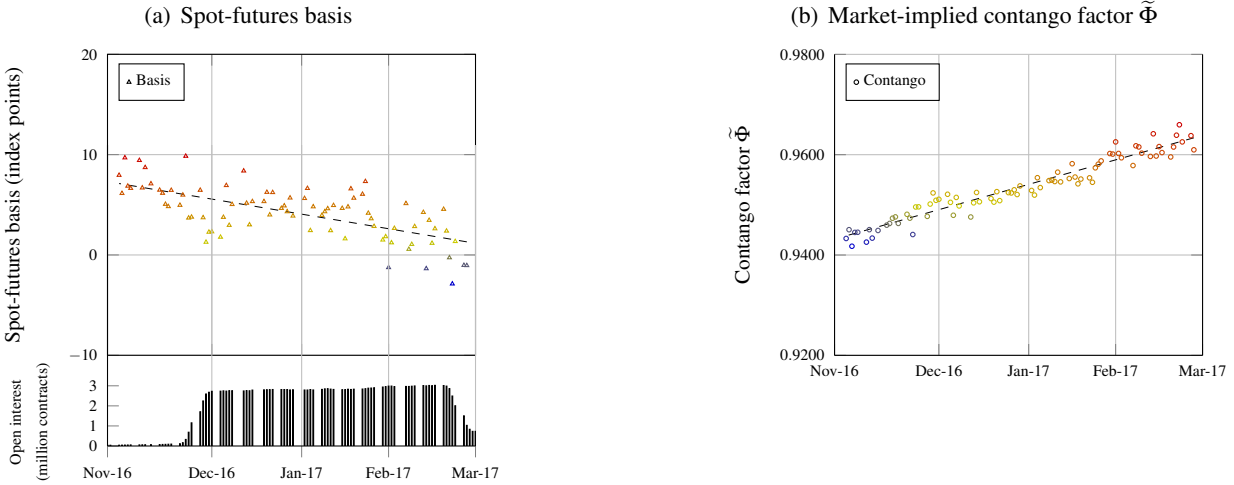
¹⁹To substantiate this intuition more rigorously, assume without loss of generality a small, $\tau_a \approx T - t$, and $\Delta r = v\sqrt{3\Delta t}$. We can assess the relative magnitude of the two terms in Equation (15) by approximating their ratio as follows:

$$\frac{v(T-t) \sum_{i=t}^{T-1} \frac{S_i B_T}{B_i(T)}}{(\tilde{E}[\Phi] - 1) \sqrt{3\Delta t} \sum_{i=t}^{T-1} \frac{\tilde{E}_i[S_{i+1}] B_T}{B_i(T)}} \approx \frac{v(T-t)}{(\tilde{E}[\Phi] - 1) \sqrt{3\Delta t}}.$$

The time-to-maturity effect produced by $(T - t) \uparrow \infty$ must be compensated by $\tilde{E}[\Phi]$ moving away from 1.

Figure 1. Contango factor implied from the S&P 500 futures

This figure plots the daily contango factor $\tilde{\Phi}$ (bullet) and the daily spot-futures basis (triangle) implied from the E-Mini S&P 500 futures maturing in March 2017 as functions of time. On each trading day, we have calibrated $\tilde{\Phi}$ against the closing prices of the futures contract and the cash index. The cumulated index of annual realized dividend points has provided a proxy for the costs of carrying futures contracts. Overnight, 1-week, 1-month, 2-month, and 3-month tenors of LIBOR interest rates have provided proxies for the USD money market. Constant volatility parameters have been used to diffuse the interest rate process ($\nu = 0.001$, $a = 0.1$). The S&P 500 stock index realized volatility has been measured via an EWMA historical estimator. Data source: Thomson Reuters.



distributions (10 contracts out of 24) as for the S&P 500 spot-futures basis displayed in Panel A. Although the process of calibration of $\tilde{\Phi}$ to the market appears to reduce skewness and exacerbate kurtosis, it seems not to generate systematic departures from normality.

Most importantly, we expect the contango factor to be stationary around any potential time trend since we calibrate it from a trend-stationary variable—the spot-futures basis. We follow the same testing strategy as the one used for the spot-futures basis time series. Panel B shows that the ADF test statistic τ_τ with a time trend fails to reject a unit root at the 1% level for only three contracts out of 24. The KPSS test statistic τ_τ confirms this finding by showing no rejection of the null hypothesis of stationarity. We are thus inclined to accept the trend-stationarity of the contango factor time series. Preserving the stationarity of empirical data through calibration provides reliable evidence for the robustness of the model. Moreover, the stationarity of $\tilde{\Phi}$ permits statistical inference and paves the way for further empirical studies.

3.4 The continuous contango factor

To investigate the economic linkage between the market-implied contango factor and the interest rate term structure, we have pieced together S&P 500 futures series to reconstitute the S&P 500 “continuous” futures series.²⁰ More precisely, for each trading day and each futures expiry, the contango factor has first been

²⁰Practitioners use different methodologies to create futures continuous time series for back-testing purposes. Handling the chain of futures contracts requires rolling over from one contract to the other and adjusting price gaps between contracts. Since splicing together futures would include artificial discontinuities, we construct one data sequence by connecting the futures with a liquidity-based roll method to ensure a smoother transition over roll dates.

implied from the futures and the underlying cash index closing prices. Second, market-implied contango factors have been weighted by open interest across futures expiries to get the continuous contango factor $\bar{\Phi}(t)$. As an open interest-weighted combination of the various delivery months of the S&P 500 futures, the continuous futures closely tracks every leading front-month futures while avoiding sharp discontinuities around rollover periods.

Figure 2 displays the S&P 500 continuous contango factor as a scatter plot over a sample period of monetary easing (September 2007 to December 2008) and a period of tightening monetary policy (December 2015 to December 2018). Although $\bar{\Phi}(t)$ seems more volatile just after rollover dates, it nevertheless has a low standard deviation of 0.011 (resp. 0.017) over the sample period 2007-2008 (resp. 2015-2018). The steady and rising trend-line materialized by its 10-day moving average confirms the model's robustness. Figure 2 also plots the LIBOR overnight interest rate, which serves as a proxy for the short-term spot interest rate used in the calibration process.

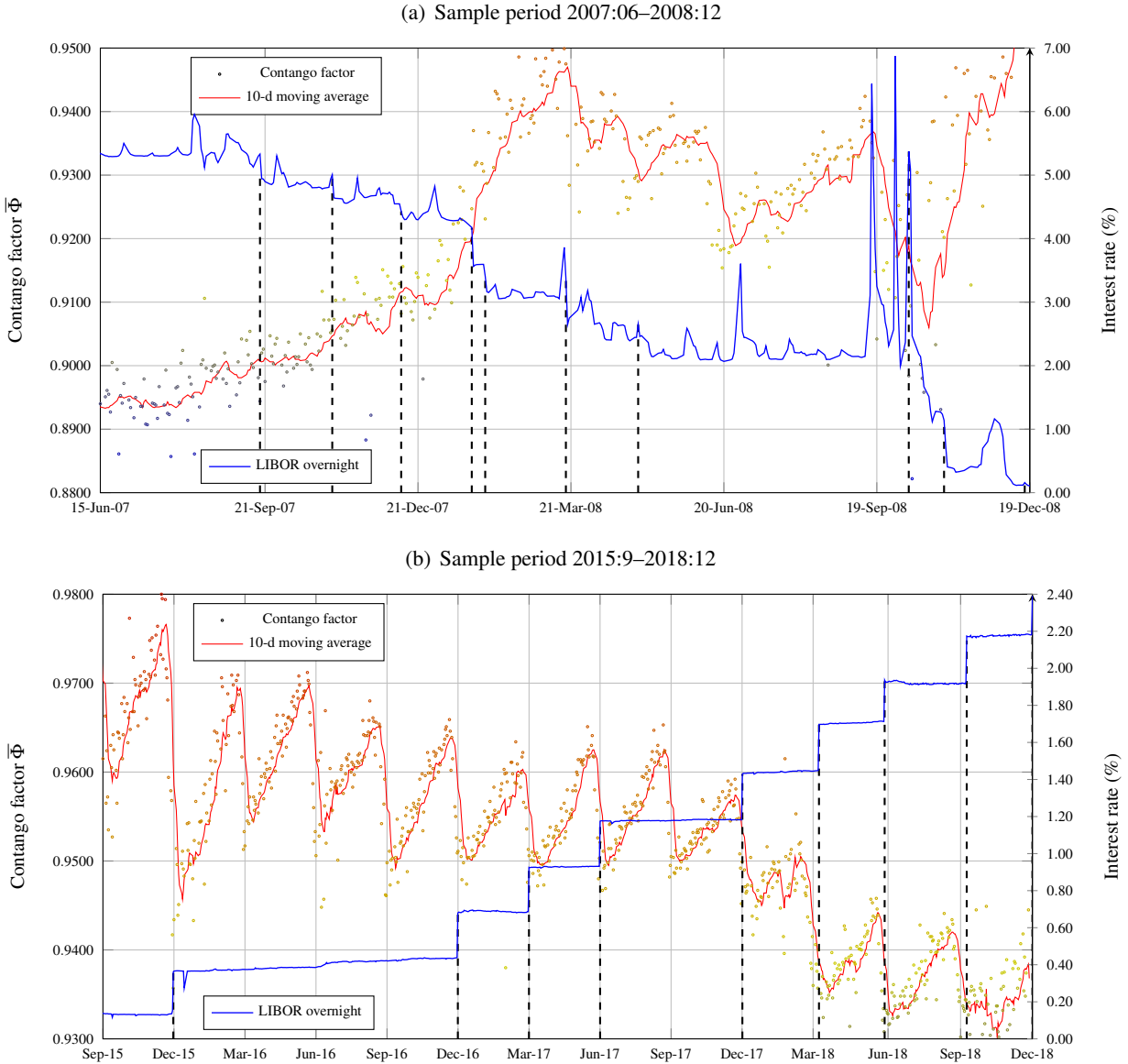
Figure 2a puts into perspective the summary statistics of Table 1. At first sight, Panel A of Table 1 could lead to interpreting 2007 as a year of healthy contango regime since the futures consistently overprices the cash index over 2007. Indeed, the negative spot-futures basis (-8.3 points on average) coheres with high carrying costs caused by interest rates above 5%. By contrast, Figure 2a highlights a low level of market-implied contango ranging from 0.89 to 0.91 over 2007. The burst of the financial crisis may explain such a low value, the asset-rate covariance remaining negative as equity markets were depressed, and interest rates boosted futures prices. This low value may also have reflected a substantial futures risk premium triggered by considerable turmoil in financial markets. In this regard, the first package of monetary policy relief in Q4 2007 translates into a surge in the contango factor during Q1 2008. In other words, had equity investors and markets not been so nervous in 2007, the futures prices would have anticipated higher cash index levels relative to the spot, translating into a more robust contango regime and a weaker futures risk premium. It is also enlightening to pinpoint the first brutal spike of the LIBOR overnight rate to 6.5% in September 2008, which corresponds to the bankruptcy of Lehman Brothers (September 15, 2008). The subsequent sharp drop in the contango factor (from 0.935 to 0.905) measures the widening of the futures risk premium caused by the financial crisis reaching its climax until the last round of monetary policy relief in mid-October 2008.

Figure 2b, by contrast, allows measuring how the context of rising interest rates translates into a higher cost of money on the margin accounts of futures holders since the U.S. Federal Reserve raised short-term interest rates nine times in a row over the sample period 2015:12–2018:12.²¹ All else being equal, this increase in the cost of money induces an increase in the futures price. Consequently, it has to come with an increase of $\bar{\Phi}(t)$ to ensure equality between the futures price and the expected future price of the cash index. Indeed, the contango factor ranges from 0.93 to 0.97, a level higher than observed during the 2007-2008 financial crisis. The macroeconomic context may explain such a change in the index-rate correlation. The continuing growth of stock markets, coupled with a new cycle of contractionary monetary policy, have for

²¹The Federal Open Market Committee (FOMC) raised the federal funds target rate on December 17, 2015 (0.25% to 0.5%), December 15, 2016 (0.5% to 0.75%), March 16, 2017 (0.75% to 1%), June 15, 2017 (1% to 1.25%), December 14, 2017 (1.25% to 1.5%), March 22, 2018 (1.5% to 1.75%), June 14, 2018 (1.75% to 2%), September 27, 2018 (2% to 2.25%), and December 20, 2018 (2.25% to 2.5%). Incidentally, FOMC meetings were generally scheduled a few trading days before oncoming S&P 500 futures expiration dates, as FOMC's regular one-day meetings are usually scheduled on Tuesdays.

Figure 2. Continuous contango factor implied from S&P 500 futures

These figures plot as a function of time the daily continuous contango factor $\bar{\Phi}(t)$ implied from E-Mini S&P 500 futures (grey) against the LIBOR overnight rate (blue). Dashed vertical lines indicate FOMC policy decisions. For each S&P 500 futures expiry, daily contango factors $\tilde{\Phi}(t, T)$ have been calibrated against the futures and cash index closing prices, and have been weighted by open interest across delivery months to obtain the daily continuous contango factor $\bar{\Phi}(t)$. The cumulated index of annual realized dividend points has provided a proxy for the costs of carrying futures contracts. Short-term tenors of LIBOR interest rates have provided proxies for the USD money market. Constant volatility parameters have been used to diffuse the interest rate process ($v = 0.001, a = 0.1$). The S&P 500 stock index realized volatility has been measured via an EWMA historical estimator. Data source: Thomson Reuters.



consequences that the negative correlation between stock indexes and interest rates tends to become less pronounced and that $\bar{\Phi}(t)$ gets closer to one.

Taking a closer look at Figure 2b enables us to distinguish two periods. During the period 2015:12–

2017:12, the Libor rates increase slowly by 80 basis points as the contango factor decreases at the same pace and never breaks the level of 0.95. For each futures contract, the time-to-maturity effect is visible (cf. Section 3.3 and footnote 19), leading to a regular “sawtooth” pattern. In contrast, during the period 2017:12–2018:12, we notice a collapse of the contango factor to 0.93 and a relative compression of the time-to-maturity effects. We attribute this decline to the macroeconomic context and the widening of the futures risk premium. We notice that the S&P 500 futures holders anticipated the Federal Reserve’s interest rate rises. After each interest rate hike, we observe a reversal in the market-implied contango trend, indicating a temporary widening of the negative index-rate correlation, which may be explained by an overshooting of investors’ anticipations.

4. Numerical Simulations

In this section, we use the methodology described in Section 2.8 to carry out numerical simulations for pricing and conducting a sensitivity analysis of futures contracts. In Appendix E.5, we discuss the pricing assumptions used in these numerical simulations in detail.

4.1 The impact of the contango factor on the futures risk premium

In our two-factor discrete-time model, we calculate the model’s theoretical futures price as the expected asset terminal value given by the hybrid lattice without stepwise discounting (see Section 2.8). It is also the expected future spot price $\tilde{E}[S_T]$ in the risk-neutral measure whose numeraire is the money market account. We then compare this theoretical futures price against the corresponding unique forward price obtained from the traditional cost-of-carry model. The latter is an unbiased estimator of the expected future spot price in the forward-neutral measure whose numeraire is the zero-coupon bond of same maturity. As a result, the futures-forward price deviation may serve as a proxy for the futures risk premium.

Table 2 reports theoretical futures prices for short-, medium- and long-term futures maturities, as well as their deviations from the forward price at each maturity as percentages. As awaited, the futures price appears to be (i) an increasing function of the contango factor, (ii) greater than the expected future spot price (contango) when $\Phi^{0,1} > 1$, (iii) less than the expected future spot price (normal backwardation) when $\Phi^{0,1} < 1$. For contango factor values close to unity, deviations from the forward prices remain less than 1%.²² As soon as the contango factor moves away from one, however, we observe differences from the traditional cost-of-carry model which are larger than 1%. More importantly, we can find theoretical futures prices below the underlying spot price for short-term maturities of less than six months, even though a substantial risk-free interest rate (3% per annum) applies for these numerical simulations.

²²To assess the magnitude of a 1% futures-forward price deviation, consider, for example, the E-mini S&P 500 futures contract. With the S&P 500 stock index around 3,000 index points (the average level over 2020), a deviation of 1% translates into a 30-point deviation in the quoted futures price. With a dollar value of USD 100 per index point, the misallocation of profit and losses between the long and short parties would be USD 3,000 per contract. With an open interest ranging between 2 and 3 million contracts (see Figure 1.a), the overall misallocation would be in the range of USD 6 to USD 9 billion, which seems far from insignificant.

Table 2. Impact of the contango factor on the futures price

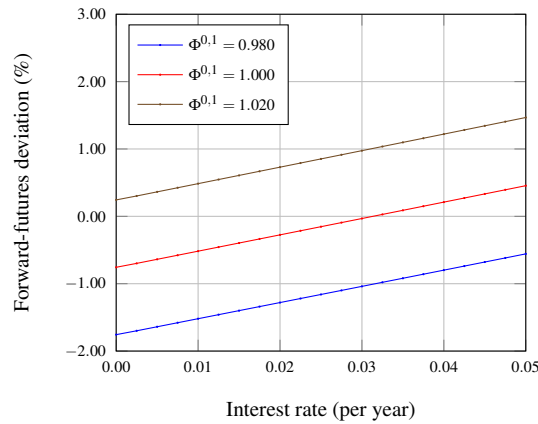
This table reports the model’s theoretical futures prices for short-, medium- and long-term contract maturities. We also report the deviation in percent from the corresponding unique forward price obtained by the traditional cost-of-carry model. Futures prices are functions of the contango factor $\Phi^{0,1}$ (assumed constant at each time-step of the simulation). The underlying asset’s initial price is $S_0 = \$100.00$ and the interest rate term structure is flat at 3% per annum. Other pricing assumptions are set out in Appendix E.5.

$\Phi^{0,1}$	Maturity of futures							
	3 months		6 months		1 year		5 years	
	Price (\$)	Dev. (%)	Price (\$)	Dev. (%)	Price (\$)	Dev. (%)	Price (\$)	Dev. (%)
0.980	99.74	(1.01)	100.44	(1.02)	102.00	(1.02)	114.95	(1.07)
0.985	99.99	(0.76)	100.69	(0.77)	102.26	(0.77)	115.24	(0.82)
0.990	100.24	(0.51)	100.95	(0.52)	102.51	(0.52)	115.53	(0.57)
0.995	100.49	(0.26)	101.20	(0.27)	102.77	(0.27)	115.82	(0.32)
1.000	100.74	(0.01)	101.46	(0.02)	103.03	(0.02)	116.12	(0.07)
1.005	100.99	0.24	101.71	0.23	103.29	0.23	116.41	0.18
1.010	101.25	0.49	101.96	0.48	103.54	0.48	116.70	0.43
1.015	101.50	0.74	102.22	0.73	103.80	0.73	116.99	0.68
1.020	101.75	0.99	102.47	0.98	104.06	0.98	117.28	0.93

Figure 3 plots the deviation of the theoretical 3-month futures price from the forward price as a function of the interest rate and for various levels of the contango factor. The level of the implicit asset-rate covariance built in the contango factor appears to have a steep impact on the degree of the forward-futures deviation. The higher the contango factor, the more beneficial the effects on the margin account of the long holder of a futures position, and the higher the forward-futures deviation. Figure 3 confirms that our model covers a broad spectrum of scenarios for the forward-futures deviation owing to the flexibility of the Φ parameter.

Figure 3. Impact of the contango factor on the forward-futures deviation

This figure plots the deviation of the 3-month futures price from the corresponding unique forward price (obtained from the cost-of-carry model) as a function of the interest rate assumed constant at each time-step of the simulation. The interest rate volatility has been set to $\nu = 0.1\%$. Other pricing assumptions are set out in Appendix E.5.



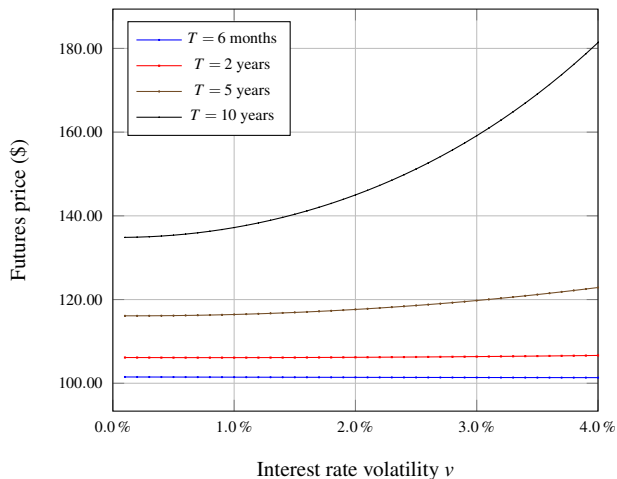
4.2 The impact of the interest rate volatility on futures prices

In a context of stochastic interest rates, we know from Cox, Ingersoll, and Ross’s theory (1981, cf. Equation (26), p. 332) that the futures price is an increasing function of the variance of interest rates. In other words, a higher interest rate volatility should translate into a higher co-movement between interest rates and asset prices, thereby pushing the futures price upward.

Figure 4 plots the futures price given by our two-factor model as a function of the interest rate volatility v . A neutral contango factor ($\Phi^{0,1} = 1$) has been chosen to run the simulations. As the CIR theory predicts, the futures price appears to be an increasing function of interest rate volatility, an effect which becomes more significant for longer-term maturities.

Figure 4. Impact of the interest rate volatility on the futures price

This figure plots the model theoretical futures price as a function of the interest rate volatility assuming a neutral contango factor $\Phi^{0,1} = 1.00$. The futures contract time to maturity T has been varied from short-term maturities (6 months) to longer-term maturities (10 years). The underlying asset’s initial price is $S_0 = \$100.00$ and the interest rate term structure is flat at 3%. Other pricing assumptions are set out in Appendix E.5.



5. Conclusions

In this article, we propose a modeling framework applicable to financial futures contracts and their derivatives, such as futures options. The pivotal parameter of the model is the contango factor Φ . This parameter captures the propensity of the underlying asset price to co-evolve with the money market interest rate. The contango factor finds itself crystallized through the daily margin calls of the futures contract. The higher (lower) the contango factor, the more expensive (cheaper) the futures price, and the more likely a contango (normal backwardation) regime to establish. Our numerical simulations indicate that the divergence from the traditional cost-of-carry model of financial futures can be significant, with price deviations above 1%, even for short-term futures contracts.

The model calibration on S&P 500 historical data highlights the role of the market’s interest rate expectations in the formation of financial futures risk premiums at low trading frequencies. Akin to the implied

volatility of option contracts, the market-implied contango factor provides market participants with a universal gauge of the level of contango. This new measure is consistent across futures markets and maturities and paves the way for further empirical studies.

Appendix A. Proof of Proposition 1

In general, the hybrid transition multiplier can always be written as the product of the interest rate transition multiplier $1 - \Delta r$ with the (conditional) transition multiplier $1 + \Delta S/S$ of the underlying asset price:

$$u_n^{j,k} = (1 + r_j - r_k) \times \tilde{\mathbb{E}} \left[1 + \frac{\Delta S}{S} \mid \Delta r = r_k - r_j \right]. \quad (\text{A1})$$

From the conditional distribution of the bivariate normal distribution, the conditional expectation $\tilde{\mathbb{E}}[\Delta S/S \mid \Delta r]$ coincides with the projection of $\Delta S/S$ onto the space spanned by the normal variable Δr and a constant:²³

$$\begin{aligned} 1 + \tilde{\mathbb{E}} \left[\frac{\Delta S}{S} \mid \Delta r \right] &= 1 + \tilde{\mathbb{E}} \left[\frac{\Delta S}{S} \right] + \text{Cov} \left[\frac{\Delta S}{S}, \Delta r \right] \times \frac{\Delta r - \tilde{\mathbb{E}}[\Delta r]}{\text{Var}[\Delta r]} \\ &\approx \left(1 + \tilde{\mathbb{E}} \left[\frac{\Delta S}{S} \right] \right) \cdot \left(1 + \text{Cov} \left[\frac{\Delta S}{S}, \Delta r \right] \times \frac{\Delta r - \tilde{\mathbb{E}}[\Delta r]}{\text{Var}[\Delta r]} \right). \end{aligned} \quad (\text{A2})$$

Inserting Equation (A2) into Equation (A1) yields Equation (6).

Appendix B. Proof of Proposition 2

- We consider a node $(n; i, j)$ at date n where i indicates that the underlying asset's bullish evolutions since the beginning of the lattice exceed the bearish ones by i , and j is the short rate index. Without loss of generality, we may assume that $i = 0$ and $j = 0$, since the demonstration would be the same with any other value of i and j . Let us assume that $\Phi_n^{0,1}$ is known. Our objective is to establish a relationship between $\Phi_n^{0,1}$ and $\Phi_n^{0,-1}$ by the absence of arbitrage opportunity.

- Our strategy is to build and immunize hybrid portfolios against combined changes in the underlying asset and the interest rate over three periods. Full hedging of the three stages onto the next period is then achieved through a non-arbitrage argument. In the sequel, we consider a generic hybrid portfolio $P = \{-Q_s, Q_B, 1\}$ with the following features:

1. selling a quantity Q_s of the underlying asset S_n , where S_n is the asset price at date n ;
2. owning a quantity Q_B of a \$1 discount bond maturing at the end of period $n + 2$;
3. owning one discount bond maturing at the end of period $n + 3$.

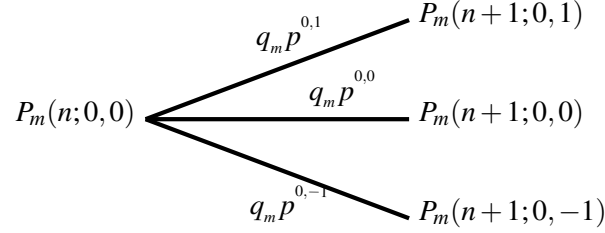
²³Here we use the well-known fact that for a Gaussian random vector (Y, X) , the conditional expectation $\mathbb{E}[Y \mid X]$ is given by $\hat{Y} := \mathbb{E}[Y] + (X - \mathbb{E}[X])\text{Cov}[X, Y]/\text{Var}[X]$. To see this, notice that the Gaussian variable $Y - \hat{Y}$ is independent from X since $\text{Cov}[X, Y - \hat{Y}] = \mathbb{E}[(X - \mathbb{E}[X])(Y - \hat{Y})] = \mathbb{E}[(X - \mathbb{E}[X])(Y - \mathbb{E}[Y])] - \mathbb{E}[(X - \mathbb{E}[X])(X - \mathbb{E}[X])]\text{Cov}[X, Y]/\text{Var}[X] = \text{Cov}[X, Y] - \text{Cov}[X, Y] = 0$ by construction. As a result we have $\mathbb{E}[Y \mid X] = \mathbb{E}[Y - \hat{Y} \mid X] + \hat{Y} = \mathbb{E}[Y - \hat{Y}] + \hat{Y} = \hat{Y}$.

The portfolio value at node $(n;0,0)$ is as follows:

$$P(n;0,0) = -Q_s S_n + \frac{Q_B}{1 + R_{n,0}(2)} + \frac{1}{1 + R_{n,0}(3)}, \quad (\text{B1})$$

where $R_{n,0}(j)$ is the yield of a discount bond maturing in j periods.²⁴ At time-step $n+1$, the portfolio may have nine different values which can easily be formulated.

• We first focus on a stable transition of the underlying asset ($i=0$) and specify a portfolio P_m . The three values of interest are on the following graph



where q_u (resp. q_m, q_d) is the conditional probability of a bullish (resp. stable, bearish) evolution of the underlying asset, and $p^{0,1}$ (resp. $p^{0,0}, p^{0,-1}$) is the interest rate bullish (resp. stable, bearish) transition probability. To immunize the portfolio P_m against interest rate movements, we solve the linear system:

$$P_m(n+1;0,0) = P_m(n+1;0,1) = P_m(n+1;0,-1) \quad (\text{B2})$$

to find the optimal asset quantity Q_s^* and the optimal bond quantity Q_B^* that equalize the three portfolio values. The solutions are:

$$Q_s^* := \frac{-1}{S_n} \cdot \frac{\frac{1+r_1}{1+r_0} \Delta_R^{0,1} + \frac{1+r_{-1}}{1+r_0} \Delta_R^{0,-1}}{\Phi_n^{0,1} - \Phi_n^{0,-1} - \frac{2\Delta r}{1+r_0}}, \quad (\text{B3})$$

and:

$$Q_B^* := \frac{\Phi_n^{0,1} - \frac{1+r_1}{1+r_0}}{\Phi_n^{0,1} - \Phi_n^{0,-1} - \frac{2\Delta r}{1+r_0}} \cdot \frac{\frac{1+r_1}{1+r_0} \Delta_R^{0,1} + \frac{1+r_{-1}}{1+r_0} \Delta_R^{0,-1}}{\Delta_r^{1,0}} + \frac{\Delta_R^{0,1}}{\Delta_r^{1,0}}, \quad (\text{B4})$$

where Δr is the interest rate tick size, and where:

$$\Delta_r^{1,0} := \frac{1}{1+r_1} - \frac{1}{1+r_0}, \quad \text{and} \quad \Delta_R^{0,\pm 1} := \frac{1}{1+R_{n+1,0}(2)} - \frac{1}{1+R_{n+1,\pm 1}(2)}. \quad (\text{B5})$$

²⁴ $R_{n,0}(j)$ is not expressed in annual rates but over j periods. In particular, $1/(1+R_{n,k}(2))$ is the value as seen at node $(n;k,i)$ of a 2-period discount bond maturing at time $(n+2)\Delta t$, and is known analytically in the case of the Hull and White (1993) model:

$$\frac{1}{1+R_{n,k}(2)} = \frac{e^{(-h_n + ar_k + v^2 \Delta t / 2) \Delta t^2}}{(1+r_k)^2}.$$

In the same way, $1/(1+R_{n,k}(3))$ is the value as seen at node $(n;k,i)$ of a 3-period discount bond maturing at time $(n+3)\Delta t$, and may be obtained as:

$$\frac{1}{1+R_{n,k}(3)} = \frac{1}{1+r_k} \left[\frac{p_n^{k,k+1}}{1+R_{n+1,k+1}(2)} + \frac{p_n^{k,k}}{1+R_{n+1,k}(2)} + \frac{p_n^{k,k-1}}{1+R_{n+1,k-1}(2)} \right].$$

Thus, the portfolio $P_m^* := \{-Q_s^* S_n, Q_B^*, 1\}$ is fully hedged at step $n + 1$ against any movement in the interest rate when the underlying asset transition is stable. Note that the immunized portfolio P_m^* depends explicitly on $\Phi_n^{0,1}$ and $\Phi_n^{0,-1}$ through the quantities Q_s^* and Q_B^* .

- We now consider two additional portfolios depending explicitly on $\Phi_n^{0,1}$ and $\Phi_n^{0,-1}$. For a bearish evolution of the underlying asset ($i = -1$), we define the portfolio:

$$P_d^* := \{-Q_s^*/d, Q_B^*, 1\}, \quad (\text{B6})$$

which is fully hedged against any movement in the interest rate by construction:

$$P_d^*(n+1; -1, 0) = P_d^*(n+1; -1, 1) = P_d^*(n+1; -1, -1). \quad (\text{B7})$$

Symmetrically, for a bullish evolution of the underlying asset ($i = 1$) we define the portfolio:

$$P_u^* := \{-Q_s^*/u, Q_B^*, 1\}, \quad (\text{B8})$$

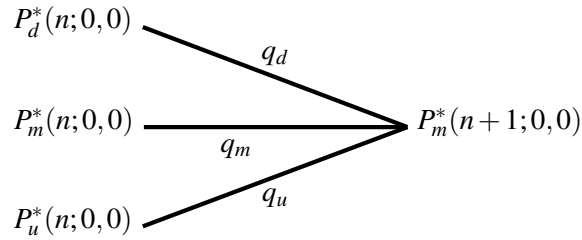
which is also fully hedged against any movement in the interest rate by construction:

$$P_u^*(n+1; 1, 0) = P_u^*(n+1; 1, 1) = P_u^*(n+1; 1, -1). \quad (\text{B9})$$

A key observation is that the three immunized portfolios P_d^* , P_m^* , and P_u^* share the same value at time-step $n + 1$ by construction:

$$P_d^*(n+1; -1, 0) = P_m^*(n+1; 0, 0) = P_u^*(n+1; 1, 0). \quad (\text{B10})$$

The following graph summarizes Equations (B2), (B7), (B9) and (B10):



- A crucial feature of this tree is that, at time-step n , only portfolios P_d^* , P_m^* and P_u^* make access possible at time-step $n + 1$ to portfolio P_m^* when moving backward. Letting D (resp., M, U) denote the probabilistic event of an up (resp. stable, down) transition from date n to date $n + 1$, we can establish the risk-neutral expectation of portfolio P_m^* at time-step n without ambiguity:

$$\begin{aligned} \tilde{\mathbb{E}}_n[P_m^*] &= \tilde{\mathbb{E}}_n[P_m^* \cdot \mathbf{1}_D] + \tilde{\mathbb{E}}_n[P_m^* \cdot \mathbf{1}_M] + \tilde{\mathbb{E}}_n[P_m^* \cdot \mathbf{1}_U] \\ &= \tilde{\mathbb{P}}[D] \cdot \tilde{\mathbb{E}}_n[P_m^* | D] + \tilde{\mathbb{P}}[M] \cdot \tilde{\mathbb{E}}_n[P_m^* | M] + \tilde{\mathbb{P}}[U] \cdot \tilde{\mathbb{E}}_n[P_m^* | U] \\ &= q_d \cdot P_d^*(n; 0, 0) + q_m \cdot P_m^*(n; 0, 0) + q_u \cdot P_u^*(n; 0, 0), \end{aligned} \quad (\text{B11})$$

where $\mathbf{1}_D$ (resp., $\mathbf{1}_M, \mathbf{1}_U$) denotes the indicator function of D (resp., M, U), and $\tilde{\mathbb{E}}_n[\cdot]$ denotes the risk-neutral

expectation seen from date n . By risk-neutral valuation, however, $\tilde{E}_n[P_m^*]$ must also be equivalent to investing in a discount bond maturing at time-step $n + 1$:

$$\tilde{E}_n[P_m^*] = \frac{P_m^*(n+1;0,0)}{1+r_0}. \quad (\text{B12})$$

Equalizing the two risk-neutral expectations given by Equations (B11) and (B12) yields:

$$q_d \cdot P_d^*(n;0,0) + q_m \cdot P_m^*(n;0,0) + q_u \cdot P_u^*(n;0,0) = \frac{P_m^*(n+1;0,0)}{1+r_0}, \quad (\text{B13})$$

where the quantities P_m^* , P_u^* and P_d^* depend explicitly on $\Phi_n^{0,1}$ and the value sought for here, that is, $\Phi_n^{0,-1}$. By substituting Equations (B3) and (B4) into Equation (B13), we can thus explicitly calculate $\Phi_n^{0,-1}$ from the pure diffusion parameters q_u (resp. q_m , q_d), the interest rate term structure $R_{n,0}(j)$, and the pre-determined parameter $\Phi_n^{0,1}$.

• To prove item (b) of Proposition 2, we note that the same line of reasoning applies more generally at any level $k \in \{-n, \dots, n\}$ of the interest rate. For negative indexes of the interest rate level ($k \leq 0$), the linear recursive relationship to be obtained is as follows:

$$\Phi_n^{k,k-1} = \frac{A_{n,k}}{C_{n,k} + D_{n,k}} + \frac{B_{n,k} + C_{n,k} + D_{n,k}}{C_{n,k} + D_{n,k}} \cdot \Phi_n^{k,k+1} - \frac{\frac{1+r_{k+1}}{1+r_k} B_{n,k} + \frac{2\Delta r}{1+r_k} (C_{n,k} + D_{n,k})}{C_{n,k} + D_{n,k}}, \quad (\text{B14})$$

where we have used $\Phi_n^{k,k} \equiv 1$, and:

$$A_{n,k} := \left(\frac{q_u^{n,k}}{u} + \frac{q_d^{n,k}}{d} + q_m^{n,k} - \frac{1}{1+r_k} \right) \left(\frac{1+r_{k+1}}{1+r_k} \Delta_R^{k,k+1} + \frac{1+r_{k-1}}{1+r_k} \Delta_R^{k,k-1} \right), \quad (\text{B15})$$

$$B_{n,k} := \left(\frac{1}{1+R_{n,k}(2)} - \frac{1}{(1+r_k)^2} \right) \frac{\frac{1+r_{k+1}}{1+r_k} \Delta_R^{k,k+1} + \frac{1+r_{k-1}}{1+r_k} \Delta_R^{k,k-1}}{\Delta_r^{k+1,k}}, \quad (\text{B16})$$

$$C_{n,k} := \left(\frac{1}{1+R_{n,k}(2)} - \frac{1}{(1+r_k)^2} \right) \frac{\Delta_R^{k,k+1}}{\Delta_r^{k+1,k}}, \quad (\text{B17})$$

$$D_{n,k} := \frac{1}{1+R_{n,k}(3)} - \frac{1}{(1+r_k)(1+R_{n+1,k}(2))}, \quad (\text{B18})$$

$$\Delta_r^{k+1,k} := \frac{1}{1+r_{k+1}} - \frac{1}{1+r_k}, \quad (\text{B19})$$

$$\Delta_R^{k,k\pm 1} := \frac{1}{1+R_{n+1,k}(2)} - \frac{1}{1+R_{n+1,k\pm 1}(2)}. \quad (\text{B20})$$

For positive indexes of the interest rate level ($k \geq 0$), the linear recursive relationship to be obtained is given by:

$$\Phi_n^{k,k+1} = \frac{-A_{n,k}}{B_{n,k} + C_{n,k} + D_{n,k}} + \frac{C_{n,k} + D_{n,k}}{B_{n,k} + C_{n,k} + D_{n,k}} \cdot \Phi_n^{k,k-1} + \frac{\frac{1+r_{k+1}}{1+r_k} B_{n,k} + \frac{2\Delta r}{1+r_k} (C_{n,k} + D_{n,k})}{B_{n,k} + C_{n,k} + D_{n,k}}. \quad (\text{B21})$$

Equations (B14) for $k \leq 0$ and (B21) for $k \geq 0$ then lead to Equation (13).

• To prove item (c) of Proposition 2, we first proceed recursively by showing that for any positive index $0 < k \leq n-1$, the number $\Phi_n^{0,k+1}$ can be deduced from the prior knowledge of $\Phi_n^{0,k}$ and $\Phi_n^{0,1}$. To show this first point, it is sufficient to use the chain rule $\Phi_n^{0,k+1} = \Phi_n^{0,k} \cdot \Phi_n^{k,k+1}$ (see Equation (11)), and to make sure that $\Phi_n^{k,k+1}$ depends *only* on $\Phi_n^{0,1}$. Indeed, Equation (13) ensures that the following linear function substitutes for $\Phi_n^{k,k+1}$ in the chain rule:

$$\Phi_n^{k,k+1} = a_{n,k} + b_{n,k} \Phi_n^{k,k-1} = a_{n,k} + \frac{b_{n,k}}{\Phi_n^{k-1,k}}, \quad (\text{B22})$$

where the second equality derives from the symmetry of the **co-movement** factor. Performing the same substitution trick as often as necessary (i.e., from index $k-1$ to index 1), the number $\Phi_n^{k-1,k}$ can be expressed as a function of $\Phi_n^{0,1}$ only. As a result, Equation (B22) ensures that $\Phi_n^{k,k+1}$ depends on $\Phi_n^{0,1}$ only.

Second, the same line of reasoning applies to prove that it is possible to recursively determine all the values of $\Phi_n^{0,k}$ for negative indexes $-n+1 \leq k < 0$ once $\Phi_n^{0,1}$ is known. Once again, all that is necessary is the chain rule $\Phi_n^{0,k-1} = \Phi_n^{0,k} \cdot \Phi_n^{k,k-1}$ (see Equation (11)), Equation (13), and the symmetry of the **co-movement** factor.

Finally, the two previous points ensure that all the numbers $\Phi_n^{0,k}$ ($-n \leq k \leq n$) can be determined recursively from the prior knowledge of $\Phi_n^{0,1}$.

Appendix C. Proof of Proposition 3

By definition, the local asset-rate covariance is given by:

$$\text{Cov} \left[\frac{\Delta S}{S}, \Delta r \right] = \tilde{\mathbb{E}} \left[\frac{\Delta S}{S} \cdot \Delta r \right] - \tilde{\mathbb{E}} \left[\frac{\Delta S}{S} \right] \cdot \tilde{\mathbb{E}} [\Delta r]. \quad (\text{C1})$$

The right-hand-side crossed expectation at node $(n; i, j)$ may be expressed using the definition (E3) of the contango process ρ as follows:

$$\sum_{k=j-1}^{j+1} p_n^{j,k} \frac{q_u^{n,j} S_0 u^i (u \rho_n^k - \rho_n^j) + q_m^{n,j} S_0 u^i (m \rho_n^k - \rho_n^j) + q_d^{n,j} S_0 u^i (d \rho_n^k - \rho_n^j)}{S_0 u^i \rho_n^j} (r_k - r_j). \quad (\text{C2})$$

Breaking down the double source of risk

$$u \rho_n^k - \rho_n^j = u \rho_n^k - u \rho_n^j + u \rho_n^j - \rho_n^j = u(\rho_n^k - \rho_n^j) + \rho_n^j(u - 1), \quad (\text{C3})$$

this crossed expectation becomes:

$$\sum_{k=j-1}^{j+1} p_n^{j,k} \frac{q_u^{n,j} u \Delta \rho_n^k + q_m^{n,j} m \Delta \rho_n^k + q_d^{n,j} d \Delta \rho_n^k}{\rho_n^j} (r_k - r_j) + \sum_{k=j-1}^{j+1} p_n^{j,k} \left(q_u^{n,j} \Delta u + q_d^{n,j} \Delta d \right) (r_k - r_j), \quad (\text{C4})$$

where $\Delta\rho_n^k := \rho_n^k - \rho_n^j$, $\Delta u := u - 1$ and $\Delta d := d - 1$. We observe now that the second sum is the product of conditional expectations $\tilde{\mathbb{E}}_j[\Delta S/S] \cdot \tilde{\mathbb{E}}_j[\Delta r]$ at node $(n; i, j)$. Substituting (C4) into the covariance definition (C1), we obtain at node $(n; i, j)$:

$$\text{Cov}_j \left[\frac{\Delta S}{S}, \Delta r \right] = \sum_{k=j-1}^{j+1} p_n^{j,k} \frac{q_u^{n,j} u + q_m^{n,j} m + q_d^{n,j} d}{\rho_n^j} \Delta \rho_n^k (r_k - r_j) \quad (\text{C5})$$

$$= \left(q_u^{n,j} u + q_m^{n,j} m + q_d^{n,j} d \right) \tilde{\mathbb{E}}_j \left[\frac{\Delta \rho}{\rho} \right] \Delta r. \quad (\text{C6})$$

The asset-rate covariance is thus stochastic since it fluctuates according to the position in the hybrid lattice. When the spatial resolution of the lattice decreases ($\Delta r \downarrow 0$), notice that the contango process coincides with the contango factor at first order: $\rho_n^j = \Phi_n^{0,j} (1 - j\Delta r + O(\Delta r^2)) = \Phi_n^{0,j} + O(\Delta r)$. As a result, the ratio $\Delta \rho / \rho$ can be further simplified:

$$\frac{\Delta \rho_n^k}{\rho_n^j} = \frac{\Phi_n^{0,j} \times \Phi_n^{j,k} - \Phi_n^{0,j}}{\Phi_n^{0,j}} = \Phi_n^{j,k} - 1 + O(\Delta r), \quad (\text{C7})$$

where we have used the contango factor chain rule (11). At first order, the local covariance becomes a function of the distance to one of the expected contango factor:

$$\text{Cov}_j \left[\frac{\Delta S}{S}, \Delta r \right] = \left(q_u^{n,j} u + q_m^{n,j} m + q_d^{n,j} d \right) \left(\tilde{\mathbb{E}}_j [\Phi] - 1 \right) \Delta r + O(\Delta r^2). \quad (\text{C8})$$

Appendix D. Proof of Proposition 4

Let $F(t, T)$ (resp. $G(t, T)$) denote the t -time futures (resp. forward) price for maturity T . Cox, Ingersoll, and Ross (1981, Proposition 9) show by absence of arbitrage that the difference between the forward and futures prices, $G(t, T) - F(t, T)$, is always equal to the value at time t of the following stream of payments:

$$B_T \sum_{i=t}^{T-1} \frac{S_i}{B_i(T)} \left(\frac{S_{i+1} - S_i}{S_i} \times \frac{B_{i+1}(T) - B_i(T)}{B_i(T)} - \left(\frac{B_{i+1}(T) - B_i(T)}{B_i(T)} \right)^2 \right), \quad (\text{D1})$$

where $B_i(T)$ is the price at time i of a default-free discount bond paying one dollar at time T , and B_T is the money market account at time T . Taking the expectation with respect to the risk-neutral measure yields:

$$F(t, T) = G(t, T) + B_T \sum_{i=t}^{T-1} \frac{S_i}{B_i(T)} \left(\text{Var} \left[\frac{\Delta B}{B} \right] - \text{Cov} \left[\frac{\Delta S}{S}, \frac{\Delta B}{B} \right] \right). \quad (\text{D2})$$

In a discrete-time setting, the discount bond percentage change writes:²⁵

$$\frac{\Delta B}{B} = -\tau_a \Delta r + O(\Delta t), \quad (\text{D3})$$

where the characteristic time $\tau_a := (1 - e^{-a(T-t)})/a$ is homogeneous to the bond duration, and $O(\Delta t)$ designates a function of maximum order Δt . Substituting for the bond percentage change yields:

$$F(t, T) = G(t, T) + B_T \sum_{i=t}^{T-1} \frac{S_i}{B_i(T)} \left(\tau_a^2 \text{Var}[\Delta r] + \tau_a \text{Cov} \left[\frac{\Delta S}{S}, \Delta r \right] \right). \quad (\text{D4})$$

Every quantity appearing on the right-hand-side is always positive, except the local asset-rate covariance which may be positive or negative. As a result, the futures price $F(t, T)$ becomes an increasing function of the asset-rate covariance.

When the spatial resolution of the lattice decreases ($\Delta r \downarrow 0$), we can insert the first-order approximation given by Equation (C5). Noticing that $\tilde{E}_i[S_{i+1}] = S_i(q_u^{n,j}u + q_m^{n,j}m + q_d^{n,j}d)$, the futures-forward difference can be rewritten as:

$$F(t, T) = G(t, T) + B_T v^2 \sum_{i=t}^{T-1} \frac{S_i \tau_a^2}{B_i(T)} + B_T \sum_{i=t}^{T-1} \frac{\tilde{E}_i[S_{i+1}] \tau_a}{B_i(T)} \left(\tilde{E}_i[\Phi_{i+1}] - 1 \right) \Delta r + O(\Delta r^2). \quad (\text{D5})$$

In particular, Equation (D5) yields the two following results.

- If rational expectations of future contango factors exceed one, that is, $\tilde{E}_i[\Phi_{i+1}] \geq 1$ for all $t \leq i < T$, then the futures price $F(t, T)$ will exceed the forward price $G(t, T)$ at first order in Δr (contango regime).
- If the forward price $G(t, T)$ is to exceed the futures price $F(t, T)$ at first order in Δr (backwardation regime), then it must be that at least one rational expectation of the future contango factor exceeds one, that is, $\tilde{E}_{i_0}[\Phi_{i_0+1}] \leq 1$ for at least one time index $t \leq i_0 < T$.

Appendix E. Lattice-based implementation of the model

E.1 Marginal evolution of the underlying asset

We discretize the underlying asset price process according to a trinomial lattice. We denote the nodes of the lattice $(n; i)$, where n is the time index, and the i index indicates that the bullish evolutions since the

²⁵To see this, recall that the process that would be followed by $B_t(T)$ in the risk-neutral world is

$$\frac{dB_t(T)}{B_t(T)} = r_t dt - v_B(t, T) d\tilde{Z}_t,$$

where the bond's price volatility is given by $v_B(t, T) := v(1 - e^{-a(T-t)})/a$ (e.g., Hull and White, 1993). Substituting the stochastic dynamics of the short rate given by Equation (1), we have:

$$\frac{dB_t(T)}{B_t(T)} = -\frac{1 - e^{-a(T-t)}}{a} dr_t - \frac{1 - e^{-a(T-t)}}{a} (h_t - ar_t) dt + r_t dt.$$

beginning of the lattice exceed the bearish ones by a number equal to i (a negative number means the bearish evolutions exceed the bullish ones). The starting point S_0 of the lattice corresponds to $n = i = 0$. For some subsequent node $(n; i)$ the extended kernel is as follows:

$$S_n(i) \begin{cases} u \cdot S_n(i) \\ m \cdot S_n(i) \\ d \cdot S_n(i) \end{cases}$$

where u (resp. m , d) is the upward (resp. stable, downward) transition multiplier. The evolution parameters are assumed to be constant over time and equal to $u = \exp(\theta\sigma\sqrt{\Delta t})$, $m = 1$ and $d = \exp(-\theta\sigma\sqrt{\Delta t})$, where the “stretch” parameter θ is higher than one to ensure consistent transition probabilities (Boyle, 1988; Hull and White, 1993).

E.2 Margin account valuation

Hull and White (1990b, 1993) make the normal short rate process discrete, according to a trinomial tree. In a discrete world, the drift of the mean-reverting process at node $(n; j)$ is formulated as $h(n\Delta t) - ar_j$, where n stands for time and j indexes the interest rate level. This arbitrage-free process becomes evident as soon as we set $h_n := h(n\Delta t)$ through an exact fit to the term structure. Considering the dynamics of the mean-reverting process and the yield to maturity of zero-coupon bonds, Hull and White (1993) find that:

$$h_n = (n+2)R_0(n+2) + \frac{v^2\Delta t}{2} + \frac{1}{\Delta t^2} \log \left(\sum_j Q_n^j e^{-2r_j\Delta t + ar_j\Delta t^2} \right), \quad (\text{E1})$$

where $R_0(n+2)$ represents the yield (per period) of a zero-coupon bond reaching maturity in $n+2$, and Q_n^j is the $(n; j)$ -th Arrow-Debreu security price, i.e., the value at time zero of the security paying a monetary unit at node $(n; j)$. Given the value of h_n and the interest rate step Δr , we move from the node $(n; j)$ to the node $(n+1; k)$ by choosing the index k such that the central branch of the lattice at $n+1$ reaches a value r_k which is as close as possible to $r_j + h_n - ar_j$. The two other values for the short rate at time-step $n+1$ may be deduced from r_k respectively by adding and subtracting the tick size Δr .

Let $p_n^{j,k-1}$, $p_n^{j,k}$, and $p_n^{j,k+1}$ be the risk-neutral probabilities of movements to nodes $(n+1; k-1)$, $(n+1; k)$, and $(n+1; k+1)$. If movements within the interest rate lattice are to respect moments of order 1 and order 2 of the short rate process, these probabilities are as follows:

$$\begin{cases} p_n^{j,k+1} = \frac{v^2\Delta t}{2\Delta r^2} + \frac{\eta^2}{2\Delta r^2} + \frac{\eta}{2\Delta r}, \\ p_n^{j,k} = 1 - \frac{v^2\Delta t}{\Delta r^2} - \frac{\eta^2}{\Delta r^2}, \\ p_n^{j,k-1} = \frac{v^2\Delta t}{2\Delta r^2} + \frac{\eta^2}{2\Delta r^2} - \frac{\eta}{2\Delta r}, \end{cases} \quad (\text{E2})$$

where $\eta := (j-k)\Delta r + (h_n - ar_j)\Delta t$. These probabilities must be positive or nil; this condition leads to a range of acceptable values for the interest-rate tick Δr .

E.3 Geometry of the hybrid lattice

We first encapsulate the asset-rate sensitivity into a new auxiliary process.

Definition 3 (Contango process). *The contango process ρ_n^k is defined from the interest rate process and the contango factor as:*

$$\rho_n^k := \Phi_n^{0,k} \cdot \frac{1+r_0}{1+r_k}. \quad (\text{E3})$$

The amplitude of the contango process captures the propensity of the underlying asset price to co-evolve with the margin account funding cost.

We describe any path joining the hybrid lattice's root to node $(n; i, k)$ as a sequence of integer pairs $\{(0, 0); (i_1, k_1); \dots; (i_{n-1}, k_{n-1}); (i_n, k)\}$, where the i s are asset price transitions in $\{0, \pm 1\}$, the k s are contiguous interest rate levels in $\{-n, \dots, n\}$, and the bullish evolutions since the beginning of the hybrid lattice exceed the bearish ones by a (signed) integer i equal to $i_1 + \dots + i_n$. Now rewrite the stock price history along this path as follows:

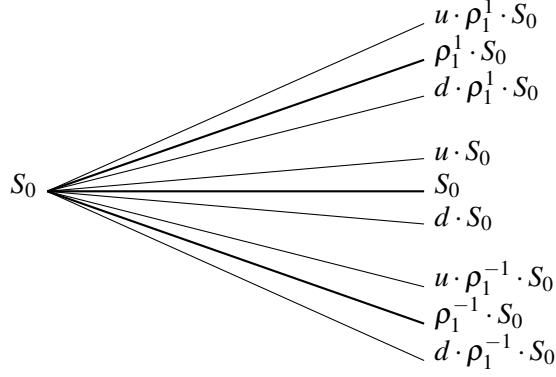
$$\begin{aligned} \frac{S_n}{S_0} &= \frac{S_n}{S_{n-1}} \times \dots \times \frac{S_1}{S_0} = u^{i_n} \Phi_{n-1}^{k_{n-1}, k} \frac{1+r_{k_{n-1}}}{1+r_k} \times \dots \times u^{i_1} \Phi_1^{0, k_1} \frac{1+r_0}{1+r_{k_1}} \\ &= u^i \times \Phi_1^{0, k_1} \times \dots \times \Phi_{n-1}^{k_{n-1}, k} \times \frac{1+r_0}{1+r_k}. \end{aligned} \quad (\text{E4})$$

This calculation shows that the discretized asset price process is Markov as soon as the chain rule $\Phi_n^{0,k} = \Phi_1^{0, k_1} \times \dots \times \Phi_{n-1}^{k_{n-1}, k}$ holds, which is equivalent to the recombining feature of the hybrid lattice (see Assumption 5). In this case, the set of contango factors $\{\Phi_n^{0,k}\}_{n,k}$ serves as the hybrid lattice's coordinate system and determines its geometry.

Equation (E4) enables to write the underlying asset price at any node $(n; i, k)$ in the compact form:

$$S_n^{i,k} := u^i \cdot \rho_n^k \cdot S_0, \quad (\text{E5})$$

where u^i captures the evolution due to the [asset fundamentals](#), and the contango process ρ_n^k captures all the information on the state-dependent covariance between the joint evolution of asset prices and interest rates. Equation (E5) shows that the contango process provides the hybrid lattice with its skeleton. In the case in which the money market funding cost remains constant at level r_0 , we have $\rho_1^0 \equiv 1$ and the usual values of the classical trinomial model appear in the middle of the hybrid lattice. However, as soon as the funding cost changes, the asset price lattice is far from resembling the classical trinomial model.



At this stage, it is worth emphasizing the non-explosive aspect of the model that arises from the parsimonious properties of the Hull and White short rate lattice. Indeed, due to the mean reverting feature of the short rate dynamics, the lattice unfolds like a “tube” rather than a cone. At time-step n , the total number of scenarios is $(2n + 1)j_n$, where j_n is the number of interest rate scenarios that are specific to the time-step. Hull and White (1994) show that we may choose the maximal interest rate index as $j_{max} = \lfloor 0.184/(a\Delta t) \rfloor$, a choice that ensures a bounded number of interest rate scenarios.

E.4 Transition probabilities within the hybrid lattice

It is now possible to establish the transition probabilities from the scenario $(n; i, j)$ to the nine following scenarios that arise in the hybrid lattice at time-step $n + 1$. The underlying asset price movement is assumed to result from two distinct effects —one arising from its **fundamentals**, and the other stemming from the money market interest rate. The probabilities characterizing the interest rate’s movement are independent of the stock price movement, but the probability of the evolution of the **asset fundamentals** is assumed to depend on the level of the interest rate r at time-step n . Let $q_u^{n,j}$ (resp. $q_m^{n,j}, q_d^{n,j}$) be the conditional probability of a bullish (resp. stable, bearish) evolution of the **asset fundamentals** when going from time-step n to time-step $n + 1$ conditionally upon the interest rate being r_j over this period.

The transition probabilities specific to each of the scenarios at time-step $n + 1$ are the product of the probability characterizing the interest rate’s movement and the conditional probability of a bullish (or stable, or bearish) evolution of the stock’s **fundamentals** when the interest rate movement is given. As a result, probabilities specific to each of the nine scenarios transitioning from r_j to r_k appear as the products of the three conditional probabilities $q_u^{n,j}, q_m^{n,j}$, and $q_d^{n,j}$ with the three probabilities $p_n^{j,k-1}, p_n^{j,k}$, and $p_n^{j,k+1}$. The next proposition provides the values of these three conditional probabilities.

PROPOSITION 5 (Transition probabilities). *When the interest rate stays at the level j between n and $n + 1$,*

the marginal risk-neutral transition probabilities of the asset price lattice are given by:

$$\begin{cases} q_u^{n,j} = \frac{V + M^2 + dm_j^2 - M(d+1)m_j}{m_j^2(u-1)(u-d)}, \\ q_d^{n,j} = \frac{V + M^2 + um_j^2 - M(u+1)m_j}{m_j^2(1-d)(u-d)}, \\ q_m^{n,j} = 1 - \frac{V + M^2 + (u+d-1)m_j^2 - M(u+d)m_j}{m_j^2(1-d)(u-1)}, \end{cases} \quad (\text{E6})$$

where $M := (1 + r_j - q)\Delta t$ is the conditional mean of the asset price process in the money market account numeraire, $V := \sigma^2\Delta t$ is the conditional variance of the asset price process, and $m_j := \Phi_n^{0,j}/\Phi_{n-1}^{0,j}$ is the stable transition multiplier within the lattice at level j . In the non-hybrid case (i.e., $j = 0$, $m_j = 1$) we recover the standard trinomial transition probabilities of Boyle (1988).

Proof. The result comes directly from the observation that at node $(n; i, j)$, in the case where the interest rate stays at the level j between time-steps n and $n + 1$, the marginal probabilities should match the first two moments of the underlying asset price diffusion. First, the probabilities sum to one:

$$q_u^{n,j} + q_m^{n,j} + q_d^{n,j} = 1. \quad (\text{E7})$$

Second, the mean of the discrete distribution is equal to the mean of the continuous lognormal distribution:

$$q_u^{n,j} u_n^{j,j} S_n^{i,j} + q_d^{n,j} d_n^{j,j} S_n^{i,j} + q_m^{n,j} m_n^{j,j} S_n^{i,j} = M_j S_n^{i,j}, \quad (\text{E8})$$

where the evolution coefficients within the lattice at level j are given by:²⁶

$$\begin{cases} u_n^{j,j} = u \cdot m_n^{j,j}, \\ m_n^{j,j} = \Phi_n^{0,j}/\Phi_{n-1}^{0,j}, \\ d_n^{j,j} = d \cdot m_n^{j,j}, \end{cases} \quad (\text{E9})$$

and where the conditional mean of the asset price process is driven by the growth rate in the money market account:

$$M_j := \frac{\tilde{\mathbb{E}}[S_{n+1}^{i,j} | S_n^{i,j}]}{S_n^{i,j}} = (1 + r_j - q)\Delta t. \quad (\text{E10})$$

Third, the variance of the discrete distribution is equal to the variance of the continuous distribution:

$$q_u^{n,j} (S_n^{i,j})^2 [(u_n^{j,j})^2 - M_j^2] + q_d^{n,j} (S_n^{i,j})^2 [(d_n^{j,j})^2 - M_j^2] + q_m^{n,j} (S_n^{i,j})^2 [(m_n^{j,j})^2 - M_j^2] = V_j (S_n^{i,j})^2, \quad (\text{E11})$$

²⁶These relationships are simple consequences of the $\Phi_n^{0,j}$'s being a coordinate system for the hybrid lattice. For example, the lattice's recombination (Assumption 5) imposes that $S_n^{i,j} = m_n^{j,j} \cdot S_{n-1}^{i,j}$, which leads to $u^i S_0 \Phi_n^{0,j} = m_n^{j,j} \cdot u^i S_0 \Phi_{n-1}^{0,j}$ after substitution of Equations (E5) and (E3), and thus to $m_n^{j,j} = \Phi_n^{0,j}/\Phi_{n-1}^{0,j}$.

where the conditional variance is given by:

$$V_j := \frac{\text{Var} \left[S_{n+1}^{i,j} | S_n^{i,j} \right]}{\left(S_n^{i,j} \right)^2} = \sigma^2 \Delta t. \quad (\text{E12})$$

Dividing the second equation (E8) by $S_n^{i,j}$ and the third equation (E11) by $\left(S_n^{i,j} \right)^2$, and reorganizing (E11), we obtain:

$$\begin{cases} q_u^{n,j} + q_m^{n,j} + q_d^{n,j} = 1, \\ q_u^{n,j} m_j u + q_d^{n,j} m_j d + q_m^{n,j} m_j = M_j, \\ q_u^{n,j} m_j^2 u^2 + q_d^{n,j} m_j^2 d^2 + q_m^{n,j} m_j^2 = V_j + M_j^2, \end{cases} \quad (\text{E13})$$

where $m_j := m_n^{j,j}$. The first equation can be used to remove $q_m^{n,j} m_j$ from the last two equations, and we are left with solving the following linear system:

$$\begin{cases} q_u^{n,j} m_j (u-1) + q_d^{n,j} m_j (d-1) = M_j - m_j, \\ q_u^{n,j} m_j^2 (u^2-1) + q_d^{n,j} m_j^2 (d^2-1) = V_j + M_j^2 - m_j^2, \end{cases} \quad (\text{E14})$$

the solution of which is given by:

$$\begin{cases} q_u^{n,j} = \frac{u(V_j + M_j^2 - m_j M_j) - m_j(M_j - m_j)}{m_j^2(u-1)(u^2-1)}, \\ q_d^{n,j} = \frac{u^2(V_j + M_j^2 - m_j M_j) - u^3 m_j(M_j - m_j)}{m_j^2(u-1)(u^2-1)}. \end{cases} \quad (\text{E15})$$

Noticing that $ud = 1$, Equations (E6) of Proposition 5 are then easily obtained. Note that in the non-hybrid case (i.e., $j = 0, m_j = 1$) we recover the standard trinomial transition probabilities from Boyle (1988):

$$\begin{cases} q_u = \frac{(V + M^2 - M)u - (M - 1)}{(u-1)(u^2-1)}, \\ q_d = \frac{u^2(V + M^2 - M) - u^3(M - 1)}{(u-1)(u^2-1)}. \end{cases} \quad (\text{E16})$$

□

E.5 Pricing assumptions used in this paper

As the size of the hybrid lattice grows only linearly with the time variable, we are able to use a time resolution as thin as a day for shorter-term maturities (such as 3-month futures contracts) and no longer than a week for longer-term maturities such as 5-year futures contracts (with a simulation covering 260 weekly periods). We optimize the spatial resolution with a stretch parameter of $\theta = \sqrt{3}$ as described in Boyle (1988) and Hull and White (1990a). The spatial step Δr used for the interest rate is then equal to $v\sqrt{3\Delta t}$, and the underlying asset transition multiplier u is equal to $\exp(\sigma\sqrt{3\Delta t})$.

Table 3 lists the pricing assumptions and market data used in the numerical simulations. We use a flat interest rate curve set at 3% per annum. Without loss of generality, we assume no discrete cash dividend payment paid out by the underlying asset.

Table 3. Pricing assumptions used in numerical simulations

Parameter	Description	Value
S_0	Underlying asset initial price	\$100.00
σ	Underlying asset volatility (annualized)	20.0%
q	Underlying asset dividend yield & repo rate	0%
r	Risk-free interest rate	3.00% per annum
a	Interest rate mean reversion speed	0.1
v	Interest rate normal volatility (annualized)	0.001

References

- Alexander, C., Kaeck, A., and A. Sumawong. 2019. A parsimonious parametric model for generating margin requirements for futures. *European Journal of Operational Research* 273:31–43.
- Barberis, N., Shleifer, A., and Wurgler, J. 2005. Comovement. *Journal of Financial Economics* 75:283–317.
- Bawa, V.S., and Lindenberg, E.B. 1977. Capital Market Equilibrium in a Mean-Lower Partial Moment Framework. *Journal of Financial Economics* 5:189–200.
- Black, F. 1976. The Pricing of Commodity Contracts. *Journal of Financial Economics* 3:167–179.
- Black, F., and P. Karasinski. 1991. Bond and Option Pricing When Short Rates Are Lognormal. *Financial Analysts Journal* 47:52–59.
- Black, F., and M. Scholes. 1973. The Pricing of Options and Corporate Liabilities. *Journal of Political Economy* 81:637–654.
- Boyle, P. 1986. Option Valuation Using a Three-Jump Process. *International Options Journal* 3:7–12.
- Boyle, P. 1988. A Lattice Framework for Option Pricing with Two State Variables. *Journal of Financial and Quantitative Analysis* 23:1–12.
- Brandt, M.W., and F.X. Diebold. 2006. A No-Arbitrage Approach to Range-Based Estimation of Return Covariances and Correlations. *Journal of Business* 79:61–74.
- Buraschi, A., P. Porchia, and F. Trojani. 2010. Correlation Risk and Optimal Portfolio Choice. *Journal of Finance* 65:393–240.
- Campbell, J.Y. (1991) A Variance Decomposition for Stock Returns, *Economic Journal* **101**, 157–179.
- Campbell, J.Y. and Shiller, R.J. (1988a) The Dividend-Price Ratio and Expectations of Future Dividends and Discount Factors, *Review of Financial Studies* **1**, 195–228.
- Campbell, J.Y. and Shiller, R.J. (1988b) Stock Prices, Earnings, and Expected Dividends, *Journal of Finance* **43**, 661–676.
- Casassus, J., and P. Collin-Dufresne. 2005. Stochastic Convenience Yield Implied from Commodity Futures and Interest Rates. *Journal of Finance* 60:2283–2331.

- Casassus, J., P. Liu, and K. Tang. 2013. Economic Linkages, Relative Scarcity, and Commodity Futures Returns. *Review of Financial Studies* 26:1324–1362.
- Chen, L. and Zhao, X. 2009. Return Decomposition, *Review of Financial Studies* 22:5213–5249.
- Chen, L., Da, Z., and Zhao, X. 2013. What Drives Stock Price Movements?, *Review of Financial Studies* 26: 841–876.
- Chen, S.-S., Lee, C.-F., and Shrestha, K. 2003. Futures Hedge Ratios: A Review. *The Quarterly Review of Economics and Finance* 43:433–465.
- Chiu, M.C., H.Y. Wong, and J. Zhao. 2015. Commodity Derivatives Pricing with Cointegration and Stochastic Covariances. *European Journal of Operational Research* 246:476–486.
- Chow, Y.-F., M. McAleer, and J.M. Sequeira. 2000. Pricing of Forward and Futures Contracts. *Journal of Economic Surveys* 14:215–253.
- Cootner, P.H. 1960 Returns to Speculators: Telser versus Keynes. *Journal of Political Economy* 68:396–404.
- Cox, J.C., J.E. Ingersoll, and S.A. Ross. 1981. The Relation between Forward Prices and Futures Prices. *Journal of Financial Economics* 9:321–346.
- Cox, J.C., J.E. Ingersoll, and S.A. Ross. 1985. A Theory of the Term Structure of Interest Rates. *Econometrica* 53:385–407.
- D’Agostino, R.B., and Pearson, E.S. (1973) Tests for Departure from Normality. Empirical Results for the Distributions of b_2 and $\sqrt{b_1}$. *Biometrika* 60, 613–622.
- Dickey, D.A. and Fuller, W.A. (1981) Likelihood Ratio Statistics for Autoregressive Time Series with a Unit Root, *Econometrica* 49, 1057–1072.
- Driessen, J., P.J. Maenhout, and G. Vilkov. 2009. The Price of Correlation Risk: Evidence from Equity Options. *Journal of Finance* 64:1377–1406.
- Dupire, B. (1994) Pricing with a smile, *Risk*, 18–20.
- Fama, E.F., and K.R. French. 1987. Commodity Futures Prices: Some Evidence on Forecast Power, Premiums, and the Theory of Storage. *Journal of Business* 60, 55–73.
- Fishburn, P.C. 1977. Mean-Risk Analysis with Risk Associated with Below-Target Returns, *American Economic Review* 67:116–126.
- French, K.R. 1983, A Comparison of Futures and Forward Prices. *Journal of Financial Economics* 12, 311–342.
- Gatheral, J. (2006) *The Volatility Surface: A Practitioner’s Guide*. John Wiley & Sons, Hoboken.
- Gorton, G.B., F. Hayashi, and K.G. Rouwenhorst. (2012) The Fundamentals of Commodity Futures Returns. *Review of Finance* 17:35–105.
- Gourieroux, C., J. Jasiak, and R. Sufana. 2009. The Wishart Autoregressive Process of Multivariate Stochastic Volatility. *Journal of Econometrics* 150:167–181.
- Harrison, J.M., and S.R. Pliska. 1981. Martingales and Stochastic Integrals in the Theory of Continuous Trading. *Stochastic Processes and their Applications* 11:215–260.
- Heath, D., R.A. Jarrow, and A. Morton. 1992. Bond Pricing and the Term Structure of Interest Rates: A New Methodology. *Econometrica* 60:77–105.
- Hecht, P., and Vuolteenaho, T. (2006) Explaining Returns with Cash-Flow Proxies, *Review of Financial Studies* 19, 159–194.
- Hemler, M.L., and F.A. Longstaff. 1991. General Equilibrium Stock Index Futures Prices: Theory and Em-

- pirical Evidence. *Journal of Financial and Quantitative Analysis* 26:287–308.
- Heston, S.L., M. Loewenstein, and G.A. Willard. 2007. Options and Bubbles. *Review of Financial Studies* 20: 359–390.
- Hilliard, J.E., and J. Reis. 1998. Valuation of Commodity Futures and Options under Stochastic Convenience Yields, Interest Rates, and Jump Diffusions in the Spot. *Journal of Financial and Quantitative Analysis* 33: 61–86.
- Hull, J., and A. White. 1990a. Valuing Derivative Securities Using the Explicit Finite Difference Method. *Journal of Financial and Quantitative Analysis* 25:87–100.
- Hull, J., and A. White. 1990b. Pricing Interest-Rate Derivative Securities. *Review of Financial Studies* 3: 573–592.
- Hull, J., and A. White. 1993. One Factor Interest Rate Models and the Valuation of Interest Rate Derivative Securities. *Journal of Financial and Quantitative Analysis* 28:235–254.
- Hull, J., and A. White. 1994. Numerical Procedures for Implementing Term Structure Models I: Single-Factor Models. *Journal of Derivatives* 2:7–16.
- Jarrow, R.A., and G.S. Oldfield. 1981. Forward Contracts and Futures Contracts. *Journal of Financial Economics* 9:373–382.
- Kaldor, N. 1939. Speculation and Economic Stability. *Review of Economic Studies* 7:1–27.
- Keynes, J.M. 1930. *A Treatise on Money*, Vol. 2, London: MacMillan.
- Kolb, R.W. 1992. Is Normal Backwardation Normal? *Journal of Futures Markets* 12:75–91.
- Kwiatkowski, D., Phillips, P.C.B., Schmidt, P., and Shin, Y. (1992) Testing the Null Hypothesis of Stationarity Against the Alternative of a Unit Root: How Sure Are We That Economic Time Series Have a Unit Root? *Journal of Econometrics* 54, 159—178.
- Lam, K., Yu, P.L.H., and P.H. Lee. 2010. A margin scheme that advises on when to change required margin. *European Journal of Operational Research* 207:524–530.
- Laws, J., and J. Thomson. 2004. The efficiency of financial futures markets: Tests of prediction accuracy. *European Journal of Operational Research* 155:284–298.
- Lien, D., and Tse, Y.K. (1998) Hedging Time-Varying Downside Risk, *Journal of Futures Markets* 22, 705–722.
- Lien, D., and Tse, Y.K. (2002) Some Recent Developments in Futures Hedging, *Journal of Economic Surveys* 16, 357–396.
- Longin, F., and B. Solnik. 2001. Extreme Correlation of International Equity Markets. *Journal of Finance* 56: 649–676.
- Miltersen, K.R., and E.S. Schwartz. 1998. Pricing of Options on Commodity Futures with Stochastic Term Structure of Convenience Yields and Interest Rates. *Journal of Financial and Quantitative Analysis* 33: 33–59.
- Nelson, D.B., and K. Ramaswamy. 1990. Simple Binomial Processes as Diffusion Approximations in Financial Models. *The Review of Financial Studies* 3:393–430.
- Ramaswamy, S., and S.M. Sundaresan. 1985. The Valuation of Options on Futures Contracts *Journal of Finance* 40:1319–1340.
- Routledge, B.R., D.J. Seppi, and C.S. Spatt. 2000. Equilibrium Forward Curves for Commodities. *Journal of Finance* 55:1297–1338.

- Schwartz, E.S. 1997. The Stochastic Behavior of Commodity Prices: Implications for Valuation and Hedging. *Journal of Finance* 52:923–973.
- Vasicek, O. 1977. An Equilibrium Characterization of the Term Structure. *Journal of Financial Economics* 5: 177–188.
- Whitelaw, R.F. 1994. Time Variations and Covariations in the Expectation and Volatility of Stock Market Returns. *Journal of Finance* 49:515–541.
- Working, H. 1948. Theory of the Inverse Carrying Charge in Futures Markets. *Journal of Farm Economics* 30:1–28.
- Working, H. 1949. The Theory of the Price of Storage. *American Economic Review* 39:1254–1262.
- Vuolteenaho, T. (2002) What Drives Firm-Level Stock Returns?, *Journal of Finance* 57, 233–264.
- Veldkamp, L.L. (2006) Information Markets and the Comovement of Asset Prices, *Review of Economic Studies* 73:823–845.